HISTORICAL BIOLOGY
2025, VOL. 37, NO. 11, 2407–2424
https://doi.org/10.1080/08912963.2022.2139180

Taylor & Francis
Taylor & Francis Group

New discovery of a late Middle Pleistocene mammalian fauna in Ganxian Cave, Southern China

Hua Liang[a], Wei Liao[a], Qingfeng Shao[b], Qiong Chen[a], Chun Tian[a], Yanyan Yao[a], Jinyan Li[c] and Wei Wang[a]

[a]Institute of Cultural Heritage, Shandong University, Qingdao, China; [b]College of Geographical Science, Nanjing Normal University, Nanjing, China; [c]Tiandong County Museum, Tiandong, China

ABSTRACT

This report describes fossils recovered from Ganxian Cave in 2008 and 2018 by the Natural History Museum and Anthropology Museum of Guangxi. The cave sedimentary fill yielded rich mammalian fossils consisting mainly of isolated teeth of medium- to large-sized mammals (Primates, Proboscidea, Perissodactyla, Carnivora, Rodentia, Artiodactyla) of typical '*Ailuropoda-Stegodon*' fauna, (e.g. *Stegodon orientalis, Ailuropoda baconi, Pongo weidenreichi, Tapirus sinensis, Megatapirus augustus, Crocuta ultima*), and more numerous extant species belonging to 28 taxa in total. The biochronological age of the fauna agreed with the age estimates obtained using Uranium–series and coupled ESR/U-series dating. Collectively, these results indicate a Ganxian fossil age range of 168.9 ± 2.4 ka to 362 ± 78 ka and establish Ganxian Cave as one of the most precisely dated Middle Pleistocene fossil sites in southern China. Comparison of Ganxian fauna with Pleistocene fossil records of the well-documented faunas of southern China and southeast Asia indicates that the Asian elephant (*Elephas maximus*) probably first appeared in Ganxian Cave. Paleoenvironmental reconstruction-based analysis of the large mammalian fossil assemblage from Ganxian Cave indicates that during the late Middle Pleistocene, the habitat consisted mainly of forests with some open areas and the climate was warm and humid.

ARTICLE HISTORY
Received 15 August 2022
Accepted 19 October 2022

KEYWORDS
Large mammals; *Ailuropoda-Stegodon* fauna; late Middle Pleistocene; Ganxian; Southern China

Introduction

During the Pleistocene, the '*Ailuropoda-Stegodon*' fauna (*sensu lato*) was widely distributed from southern East Asia to mainland Southeast Asia (Patte 1928; de Terra 1938; Colbert 1943; Pope et al. 1981). The faunal association expanded latitudinally from northern China (e.g. Gongwangling in north Qinling Mountains) (Hu and Qi 1978; Qiu 2006) to Peninsula Thailand (e.g. Yai Ruak) (Suraprasit et al. 2019) (Figure 1).

Studies of Pleistocene mammalian faunal assemblages in southern China began in the 1920s (Matthew and Granger 1923; Pei 1935). Since the 1950s, scholars have discussed Pleistocene fauna biochronological sequences and proposed different evolutionary schemes (Zhou 1957; Kahlke and Hu 1961; Huang 1979; Pei 1980; Han and Xu 1985). However, due to the lack of systematic studies and geochronological analyses to confirm the validity of the '*Ailuropoda-Stegodon*' faunal complex, some scholars argued that the complex cannot be reliably used to describe the temporal and spatial evolution of the mammalian faunas in southern China (Wang et al. 2007).

Since 2000, Quaternary cave sequences obtained from the Bubing Basin and Chongzuo regions in southwest Guangxi have been systematically surveyed, excavated, and studied by researchers from the Natural History Museum of Guangxi, the Anthropology Museum of Guangxi, the Institute of Vertebrate Palaeontology and Palaeoanthropology and Shandong University. As a result, hundreds of Quaternary cave sites have been discovered and abundant mammal fossils have been collected that have enhanced our knowledge of mammal faunal evolution in southern China. Moreover, analysis of these fossils has greatly clarified evolutionary sequences of the Early Pleistocene faunas (Wang et al. 2007; 2014; 2017a; Rink et al. 2008; Jin et al. 2008; 2014; Sun et al. 2014).

Although numerous Middle Pleistocene mammal fossil sites have been found in southern China, most of them were dated using biochronological correlation. So far, only a few sites have absolute isotopic ages, such as Bailongdong (Liu et al. 2015; Han et al. 2019), Bulalishan (or Wuming) (Rink et al. 2008), Yanlidong (Yao et al. submitted), Daxin Hei Cave (Rink et al. 2008; Shao et al. 2017), Hejiang Cave (Zhang et al. 2014), Hualongdong (Wu et al. 2019), and Diaozhongyan (Liang et al. 2020; Liao et al. 2020). The well-described faunas of the Middle Pleistocene include the Bailongdong (Tong et al. 2019), the Daxin Hei Cave (Han 1982), the Hualongdong (Tong et al. 2018b), the Diaozhongyan (Liang et al. 2020), and the well-known site Yanjinggou (or Yenchingkou) (Colbert and Hooijer 1953). Regarding most of the remaining sites, only mammal lists are published. Although the mammalian fossils from Zhiren Cave have been dated to >106.2 ± 6.7 ka by U-series (Liu et al. 2010) and to ~116-106 ka by combined palaeomagnetic and OSL dating methods (Cai et al. 2017), Ge et al. (2020) suggests that the deposits at the site may actually be older, dating to 190–130 ka. Presently, our understanding of the mammal evolution in the Middle Pleistocene is insufficient, further investigation is necessary.

Here, we report a recent finding of Middle Pleistocene mammalian fossils from Ganxian Cave in the Bubing Basin, Guangxi Zhuang Autonomous Region, which will add significant data to this period in southern China and Southeast Asia.

Geological and chronological context

Ganxian Cave (23°36′7″ N, 106°59′52″ E) is located in a karst environment in the Bubing Basin (Figure 1). The cave was originally

CONTACT Wei Wang wangw@sdu.edu.cn Institute of Cultural Heritage, Shandong University, Qingdao, China
Supplemental data for this article can be accessed online at https://doi.org/10.1080/08912963.2022.2139180

Published online 06 Nov 2022

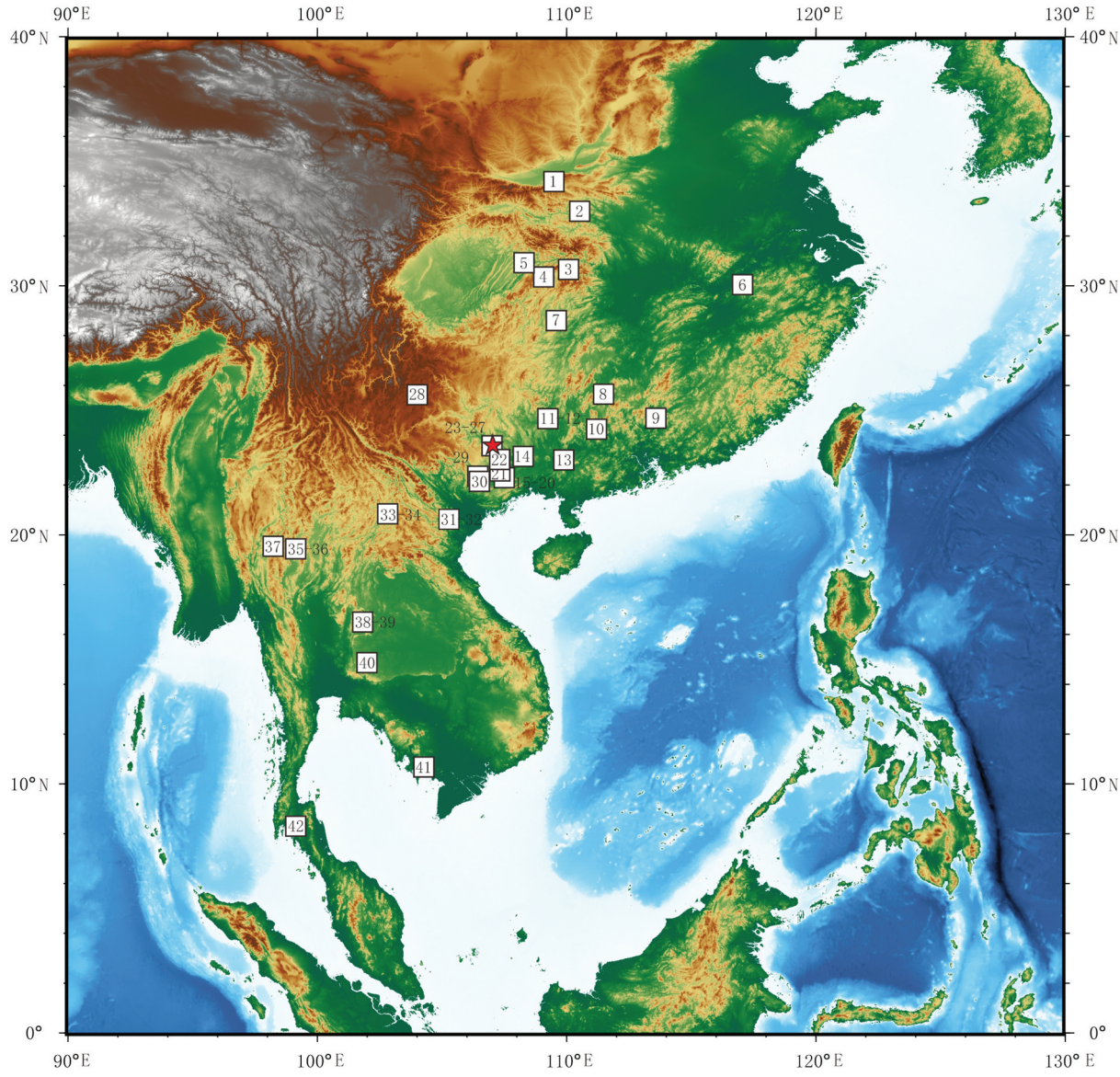

Figure 1. Location of Ganxian Cave and other Early to Late Pleistocene sites. Distribution of fossil localities in southern China: 1, Gongwangling; 2, Bailong Cave; 3, Jiangshi (Longgudong); 4, Longgupo; 5, Yanjinggou (or Yenchingkou); 6, Hualongdong; 7, Dongpaoshan; 8, Fuyan Cave; 9, Shiziyan; 10, Diaozhongyan; 11, Liucheng (*Gigantopithecus* Cave); 12, Bijiashan; 13, Mocun Cave; 14, Bulalishan; 15–20, Baikong Cave, Juyuan Cave, Sanhe Cave, Queque Cave, Hejiang Cave, Zhiren Cave; 21, Yanlidong; 22, Daxin Hei Cave; 23–27, Chuifeng Cave, Mohui Cave, Wuyun Cave, Luna Cave, Baolai Cave; 28, Panxian Dadong. Distribution of fossil localities in Vietnam: 29, Coc Muoi; 30, Tham Khuyen; 31, Duoi U'Oi; 32, Ma U'Oi; 33, Tam Hang South. Distribution of fossil localities in Laos: 34, Nam Lot. Distribution of fossil localities in Thailand: 35, Ban Fa Suai II; 36, Cave of the Monk; 37, Tham Lod; 38, Tham Wiman Nakin; 39, Tham Prakai Phet; 40, Khok Sung; 41, Boh Dambang; 42, Yai Ruak.

discovered and excavated by researchers from the Natural History Museum of Guangxi in 2008, and the second excavation was carried out by the Anthropology Museum of Guangxi in 2018. The Ganxian Cave is situated in a karst peak cluster area formed in Palaeozoic limestones (Wang et al. 2007). The cave entrance is on the north side of the mountain about 50 m above the local valley (Figure 2A). The corridor of the cave is deep and wide, about 75 m in length. At 50 m from the entrance, a branch of 20 m in length extends westerly. The sediments have been partially removed by local villagers for fertiliser. Fortunately, most of the original sediments were remaining, and a complete sedimentary sequence could be reconstructed from our excavations.

Thirteen test pits (labelled A to M) were laid out in the main passage and western branch (Figure 2F). To expose a complete sedimentary profile, pit B was excavated down to 650 cm, and other test pits were dug down to 40 to 140 cm according to various topography and residual sediments (Figure 2C). All test pits were dug down at 10 cm intervals.

Based on comparable sedimentological profiles, the stratigraphy for the 13 different test pits can be used to reconstruct a complete sedimentary sequence. Overall, the basic stratigraphy of Ganxian Cave is divided into five layers from top to bottom (Figure 2D). All mammalian teeth were recovered from a light brown sandy clay with breccia in the upper part of layer 2. The age of the mammalian fossils from Ganxian was constrained between 168.9 ± 2.4 ka and 362 ± 78 ka by U-series and coupled ESR/U-series dating methods (Liang et al. submitted).

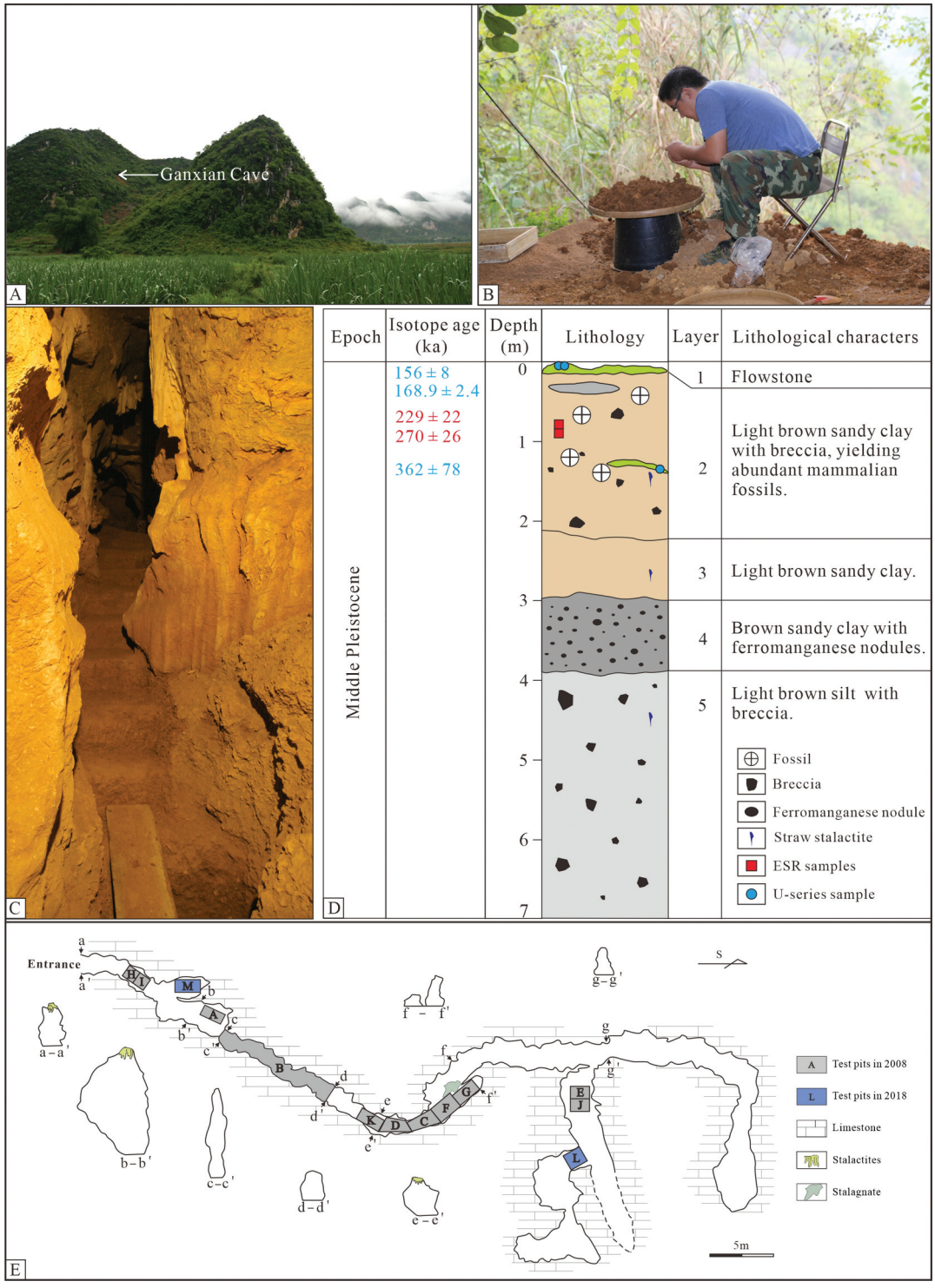

Figure 2. The Ganxian Cave. A) Landscape of the Ganxian Cave. B) Sieving and processing the smaller-sized fossils and those encased in sediment outside the Ganxian Cave. C) Test Pit B after excavation. D) The composite stratigraphy of the Ganxian Cave site. E) Plan of the Ganxian Cave with thirteen test pits. The colour of the dating results red is obtained from ESR, and blue is obtained from U-series. Abbreviations: ESR = electron spin resonance.

Materials and methods

Excavation

Our excavations concentrated on the main passage and the western branch, in an area of about 30 m^2. Pointing trowels, screwdrivers, and bamboo sticks were used to remove the soft sediments, while chisels and hammers were used to remove calcified blocks. During the excavation, medium and large sized mammalian fossils were mapped, recorded, and collected from each layer, while smaller fossils and those encased in sediment were carefully dry-sieving and processed at the entrance of the cave (Figure 2B).

Morphological descriptions and comparisons

A total number of identified specimens of more than 3000 isolated teeth of large mammals were recovered from Ganxian Cave. The

material is housed in the Natural History Museum and Anthropology Museum of Guangxi, China. The Ganxian fauna has been compared with southeast Asian faunas of known age from the Early to Late Pleistocene (Table 1). Dental nomenclature and metric measurement follow Swindler (2002) for primates, Van den Bergh (1999) for proboscideans, Yan et al. (2014) for rhinoceroses, Tong (2005) for tapirs, Jiangzuo et al. (2018a) for badgers, Jiangzuo et al. (2018b) for canids, van der Made (1996) for suids, and Suraprasit et al. (2016) and Zhang et al. (2018) for ruminants. Measurements were taken to the nearest 0.01 mm using hand-held caliper. Uppercase letters used to designate maxillary teeth, while lowercase letters are used to designate mandibular teeth. D/d prefix refers to deciduous teeth.

Results

Primates

Macaca sp.: 107 isolated teeth are attributed to *Macaca* sp., including upper and lower permanent teeth. To these specimens may be added a set of incisors and canines. The upper canine has a mesial groove (Figure 3A). The P3 (Figure 3B) and P4 (Figure 3C) both have a paracone on the buccal side and a protocone on the lingual side. The anterior transverse crista connects the paracone and protocone which divides the occlusal surface into a narrow mesial fovea and a larger distal trigon basin. The upper molars are bilophodont, showing the typical morphological pattern of *Macaca* (Figure 3D-G). On the lingual surface of the protocone, an interconulus (a remnant of cingula) can be found in most of M3 (Figure 3F-G). The p3 is sectorial, mesiodistally elongated (Figure 3H-K). The p4 has two cusps, the protoconid and metaconid. A protocristid connecting the two cusps separates the occlusal surface into narrow trigonid and slightly expanded talonid basins. Most of m3 present a *tuberculum sextum* (between the entoconid and the hypoconulid) (Figure 3N). An interconulid (a remnant of cingula) is found on the lingual surface of the protoconid in some specimens (Figure 3N).

The dimensions of the teeth are presented in Table S1. There is a large overlap with those of macaques from Longgupo (Huang and Fang 1991), Mohui Cave (Wang 2005), Juyuan Cave (Wang et al. 2017a), Longgudong (Zheng 2004), Yanlidong (Yao et al. submitted), Tham Wiman Nakin (Suraprasit et al. 2021), Tam Hang South (Bacon et al. 2011), Mocun Cave (Fan et al. 2022), Duoi U'Oi (Bacon et al. 2008), and Ma U'Oi (Bacon et al. 2004, 2006). The dimensions of M3 and m3 are larger than *M. fasicularis* and *M. mulatta*, and fall within the range of modern *M. arctoides* and *M. nemestrina* (Takai et al. 2014). We preferentially assign the Ganxian specimens to *Macaca* sp.

Trachypithecus/Presbytis sp.: A well preserved lower m3 possesses higher anterior cusp (protoconid and metaconid) than posterior cusp (Figure 3O). In the occlusal view, the hypoconulid is more developed vestibulo-lingualy (Figure 3P). As only one specimen can be identified and the morphology and dimensions (Table S2) are closed to representant of *Presbytis* and *Trachypithecus* from Juyuan Cave (Wang et al. 2017a), Yanlidong (Yao et al. submitted), and Tham Wiman Nakin (Suraprasit et al. 2021), we prefer ascribe this specimen to the subfamily colombinae indet cf. *Trachypithecus* or cf. *Presbytis*.

Table 1. Comparative mammalian fossils used in morphological description and linear metric analysis.

Fossil site	Age	Region	Source
Baikong Cave	2.58–1.95 Ma	Southern China	Jin et al. 2014; Sun et al. 2014
Longgupo	2.5–2.2 Ma	Southern China	Huang and Fang 1991; Han et al. 2017
Gigantopithecus Cave	Early Pleistocene	Southern China	Han 1987; Rink et al. 2008; Jin et al. 2008, 2014
Chuifeng Cave	1.92 ± 0.14 Ma	Southern China	Shao et al. 2014; Liao et al. (in this volume)
Mohui Cave	1.95–1.78 Ma	Southern China	Wang et al. 2005; Sun et al. 2017
Juyuan Cave	1.95–1.78 Ma	Southern China	Sun et al. 2014; Wang et al. 2017a
Longgudong	Early Pleistocene	Southern China	Zheng 2004
Sanhe Cave	~1.2 Ma	Southern China	Jin et al. 2009; Sun et al. 2014
Bijiashan	Early Pleistocene	Southern China	Han et al. 1975
Dongpaoshan	Early Pleistocene	Southern China	Wang et al. 1982
Queque Cave	1.07–0.99 Ma	Southern China	Jin et al. 2014; Sun et al. 2014
Bailongdong	0.76 ± 0.06 Ma	Southern China	Liu et al. 2015; Han et al. 2019; Tong et al. 2019
Bulalishan	481–745 ka	Southern China	Zhang et al. 1973; Rink et al. 2008
Yanlidong	~580 ka	Southern China	Yao et al. (submitted)
Tham Khuyen	>475 ka	Vietnam	Schwartz et al. 1994; Ciochon et al. 1996
Daxin Hei Cave	380–308 ka; 404–382 ka	Southern China	Han 1982; Rink et al. 2008; Shao et al. 2017
Hejiang Cave	400–320 ka	Southern China	Zhang et al. 2014
Wuyun Cave	350–200 ka; 279–76 ka	Southern China	Chen et al. 2002; Wang et al. 2007; Rink et al. 2008
Hualongdong	331–275 ka	Southern China	Tong et al. 2018b; Wu et al. 2019
Panxian Dadong	300–190 ka	Southern China	Si et al. 1993; Zhang et al. 1997; Zhang et al. 2015
Diaozhongyan	231–205 ka	Southern China	Liang et al. 2020; Liao et al. 2020
Khok Sung	217 or 130 ka	Thailand	Suraprasit et al. 2016; Duval et al. 2019
Tham Wiman Nakin	>169 ka	Thailand	Tougard 1998; Esposito et al. 1998, 2002; Suraprasit et al. 2021
Zhiren Cave	116–106 ka; 190–130 ka	Southern China	Jin et al. 2009; Liu et al. 2010; Cai et al. 2017; Ge et al. 2020
Coc Muoi	148–117 ka	Vietnam	Bacon et al. 2018a
Fuyan Cave	120–80 ka	Southern China	Li et al. 2013; Liu et al. 2015
Luna Cave	127–70 ka	Southern China	Bae et al. 2014
Tam Hang South	94–60 ka	Vietnam	Bacon et al. 2011
Nam Lot	72–86 ka	Laos	Bacon et al. 2018b
Mocun Cave	101–66 ka	Southern China	Fan et al. 2022
Duoi U'Oi	70–60 ka	Vietnam	Bacon et al. 2008
Ma U'Oi	>49 ka	Vietnam	Bacon et al. 2004, 2006
Ban Fa Suai II	55–45 ka	Thailand	Zeitoun et al. 2019
Baolai Cave	54–24 ka	Southern China	Fan et al. (submitted)
Cave of the Monk	32–19 ka	Thailand	Zeitoun et al. 2005
Boh Dambang	25–18 ka	Thailand	Bacon et al. 2018c
Tham Prakai Phet	Late Pleistocene	Thailand	Filoux et al. 2019

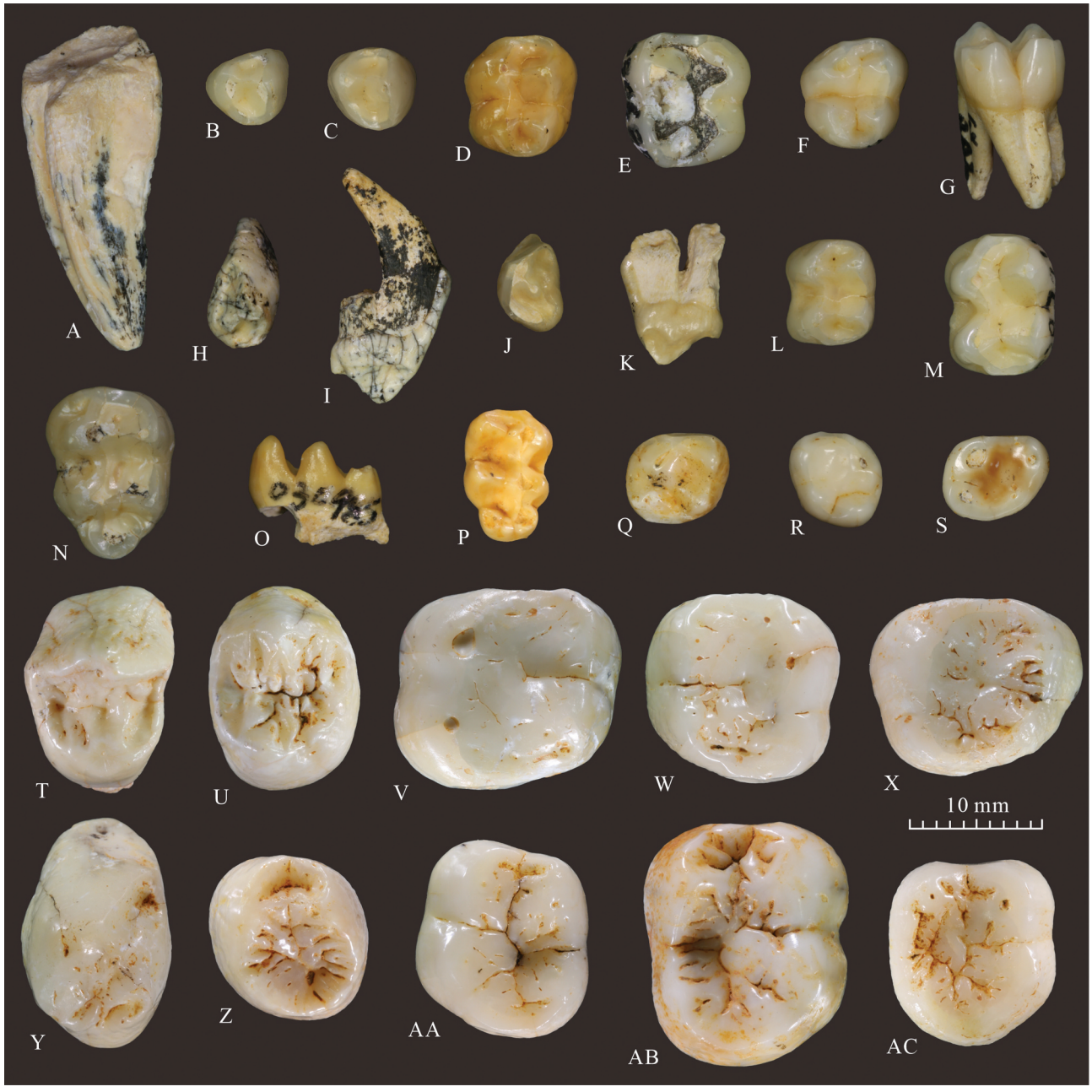

Figure 3. Primates from Ganxian Cave. *Macaca* sp.: A right C (30,441) in lingual view; B left P3 (29,745) in occlusal view; C left P4 (30,879) in occlusal view; D left M1 (30,878) in occlusal view; E right M2 (30,680) in occlusal view; F left M3 (30,679) in occlusal view; G left M3 (30,679) in lingual view; H right p3 (30,676), in occlusal view; I right p3 (30,676), in lingual view; J left p3 (29,790), in occlusal view; K left p3 (29,790), in lingual view; L left m1 (30,681) in occlusal view; M left m2 (29,744) in occlusal view; N left m3 (30,498) in occlusal view. *Trachypithecus* sp.: O right m3 (30,985) in occlusal view; P right m3 (30,985) in lingual view. *Hylobates* sp.: Q right M1 (GX-24) in occlusal view; R right M3 (GX-J5-01) in lingual view; S left M3 (GX-L3-01) in lingual view. *Pongo weidenreichi*: T right P3 (GX-25) in occlusal view; U left P4 (GX-26) in occlusal view; V left M1 (GX-27) in occlusal view; W right M2 (GX-28) in occlusal view; X left M3 (GX-29) in occlusal view; Y left p3 (GX-30) in occlusal view; Z left p4 (GX-31) in occlusal view; AA left m1 (GX-32) in occlusal view; AB right m2 (GX-33) in occlusal view; AC right m3 (GX-34) in occlusal view.

Hylobates sp.: Three upper molars and one lower molar can be attributed to the genus *Hylobates*. The upper molars display a rhombic outline (Figure 3Q-S). The protocone is the most voluminous cusp, and occupies most of the mesiolingual quadrant of the occlusal surface. A *crista obliqua* connects the protocone and the metacone. The m2 has five small and round cusps. The protocristid connecting the protoconid and metaconid is interrupted by a fine longitudinal groove. The talonid basin is smooth and unwrinkled. The dimensions of the Ganxian teeth are slightly larger than the fossil specimen from Mocun Cave (Fan et al. 2022; Table S3).

Pongo weidenreichi: One hundred and four permanent teeth and two deciduous teeth are attributed to *Pongo weidenreichi* (Liang et al. submitted). The P3 and P4 have a pointed paracone on the buccal side and a blunt protocone on the lingual side. The two cusps are separated by a deep anteroposterior valley. The upper molars display four main cusps (protocone, paracone, metacone, and hypocone). The crista obliqua connects the protocone and metacone. The p3 has a subtriangular outline in occlusal view. The p3 has a central main cusp, the protoconid. A lingual cingulum is present on all the specimens. The crown of the p4 is a slightly asymmetrical oval in occlusal

view. The p4 has two cusps, a protoconid on the buccal side and metaconid on the lingual side. A transverse crest connects the protoconid and metaconid. The lower molars have five cusps, three on the buccal side and two on the lingual side. Some sample show a typical Y-5 pattern. Overall, the morphology and dimension of the Ganxian specimens generally fall within the range of *P. weidenreichi* and can be attributed to this species. For specific morphological descriptions and dimensional comparisons, refer to Liang et al. (submitted).

Proboscidea

Elephas maximus: Three incomplete permanent teeth and a deciduous tooth, along with six isolated lamellae, were found at Ganxian. One the nearly complete dp2 preserved five lamellae (Figure 4A). The dp2 is 22.15 mm long, with a residual maximum width of 12.77 mm. The morphology and dimensions are consistent with dp2 of *E. maximus* described by Bacon et al. (2018a). One lower m2 may be determined on the remaining 12 slightly worn lamellae vertically folded in a sinusoidal way, a height/width index

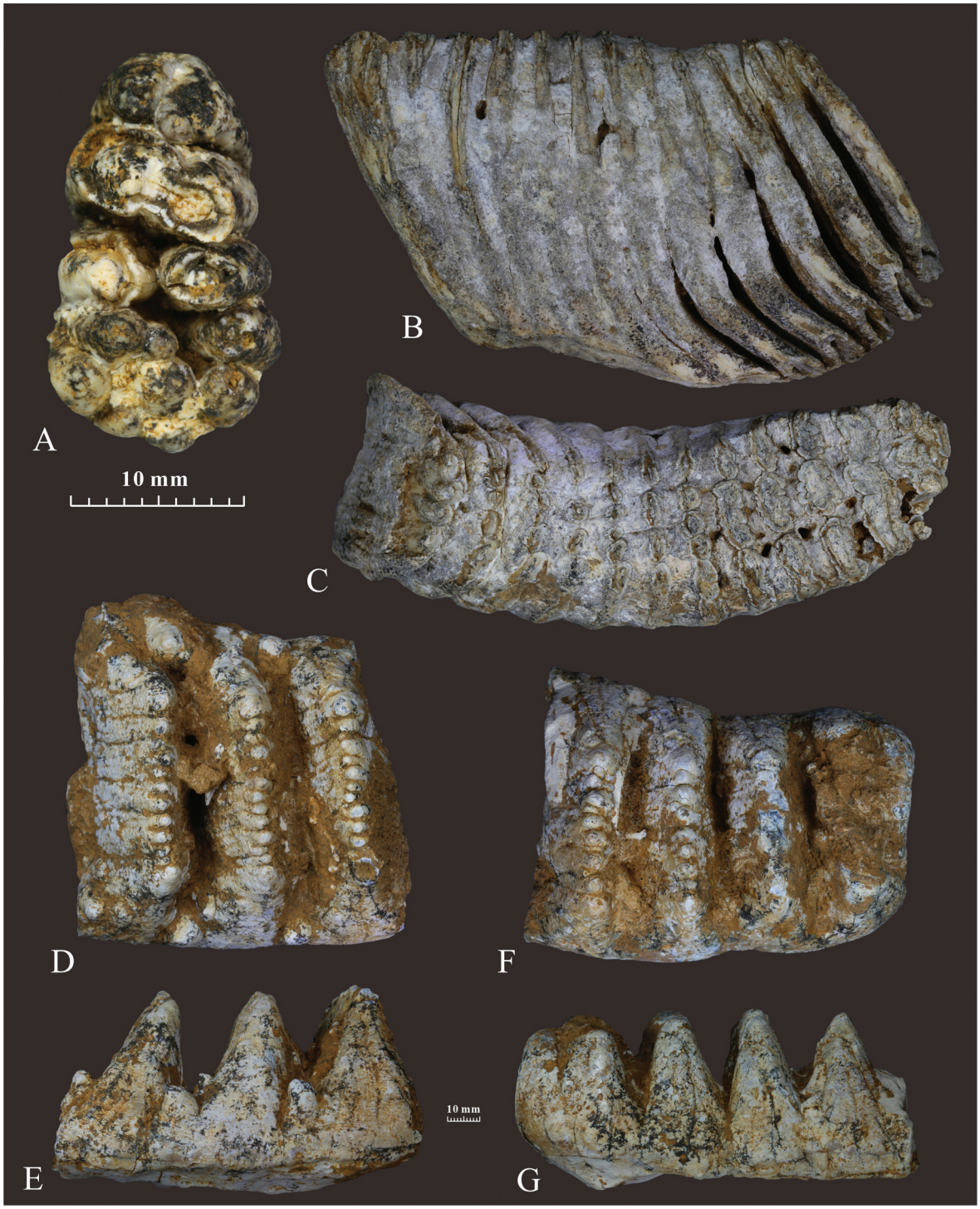

Figure 4. Proboscidea from Ganxian Cave. *Elephas maximus*: A right dp2 (GX-2) in occlusal view; B left m2 (GX-1) in buccal view; C left m2 (GX-1) in occlusal view. *Stegodon orientalis*: D right M3 (GX-3) in occlusal view; E right M3 (GX-3) in lingual view; F left m1 (GX-4) in occlusal view; G left m1 (GX-4) in buccal view.

of 208, a lamellar frequency of 9, and a maximal width of 55.26 mm (Figure 4B-C). These characteristics point to the presence of *E. maximus* rather than *E. namadicus*: the number of lamellae (for dp2, five in the Ganxian teeth versus three in *E. namadicus*; for m2, 16–21 vs 11–15); the overall dimensions of teeth and the height/width index (for m2, 208 vs 180–188) (Maglio 1973; Roth and Shoshani 1988). The morphology and dimensions of the Ganxian samples are consistent with *E. maximus* described at Coc Muoi (Bacon et al. 2018a), and supposed to be *Elephas maximus* (Bacon et al. 2018a; Table S4).

Stegodon orientalis: Thirteen remains can be assigned to *Stegodon orientalis* (two incomplete teeth; three isolated lamellae, seven tooth fragments). One M3 preserved only three ridge-shaped lophs (Figure 4D-E). These lophs are unworn. Each loph consists of 12 to 13 mammillae. Several well-developed isolated mammillae are present in the lingual and buccal sides between two lophs. The maximum width of incomplete crowns varies from 90.66 to 99.11 mm. One lower m1 preserved only four and half loghs (Figure 4F-G). The two anterior lophs are slightly worn. The maximum width of the crown is 81.84 mm. The characteristics and measurements of the Ganxian teeth are consistent with *Stegodon* described at Yangjiawan (Tong et al. 2018a; Table S4).

Perissodactyla

One DP1 and one dp1 are referred to *Rhinoceros* sp. Twenty incomplete teeth and tooth fragments are identified at the subtribe level only (Rhinocerotidae indet.).

Rhinoceros sondaicus: The DP1 crown shows a teardrop-shaped outline (Figure 5A). On the DP2, the mesostyle is posteriorly displaced (Figure 5B). The dp1s have a posterior valley that is open posteriorly and a narrower talonid (Figure 5C). The paralophid is forked, and forms a huge bulk on dp2 (Figure 5D). The posterior valet is open lingually in all specimens. The anterior extolophid groove is marked on dp3 (Figure 5E). The posterior valleys of dp3-4 and p2 are V-shaped in the lingual side. From the occlusal view, the metaconid is convex in the lingual on lower molar (Figure 5I-J). The dimensions of these specimens are close to that of *R. sondaicus* from Duoi U'Oi (Bacon et al. 2008), Tam Hang (Bacon et al. 2011), and Sanhe cave (Yan 2016) (Table S5).

Dicerorhinus sumatrensis: The DP1 displays a pentagonal outline in occlusal view (Figure 5L). The oblique external folds (paracone, mesostyle, and metacone) are present in labial view on upper premolar and molar (Figure 5N, P, and R). The M1 and M2 have an anterior constriction on the protocone, and a sigmoid protoloph (Figure 5 O and Q). The dp1 is large, possessing a wide talonid, and a shallow posterior valley, that is open on the lingual side (Figure 5S). From the occlusal view, the lingual side of the metaconid is flat on lower molar (Figure 5 U-V). The teeth morphologically resemble those of *D. sumatrensis* from *Gigantopithecus* Cave (Tong and Guérin 2009) and Duoi U'Oi (Bacon et al. 2008). The dimensions of the teeth are comparable to those fossil samples from *Gigantopithecus* Cave (Tong and Guérin 2009), Duoi U'Oi (Bacon et al. 2008), and Queque Cave (Yan 2016) (Table S6).

Tapirus sinensis: In Ganxian Cave, two permanent teeth (one P4 and one m1) are attributed to *Tapirus sinensis*. The highly worn P4 shows a square outline in occlusal view. The m1 displays a subrectangular outline, and the protolophid is wider than the hypolophid (Figure 5W). The anterior and posterior cingulum are present on the m1. The occlusal structure and dental size of the Ganxian teeth conforms to *T. sinensis* from Longgudong (Tong 2004, 2005), Bijiashan (Han et al. 1975), and Mocun Cave (Fan et al. 2022) (Table S7).

Megatapirus augustus: The large tapir from Ganxian Cave is represented by five isolated teeth. The M3 is an oblique quadrilateral in occlusal view (Figure 5X). The protocone and hypocone on the lingual side are robust than the paracone and metacone on the buccal side. The parastyle is well-developed than the metastyle. The outline of the p2 is an elongated triangular in occlusal view (Figure 5Y). The protoconid is well-developed, but not the metaconid (Figure 5Z). The m2 displays a sub-rectangular outline, and the protolophid is wider than the hypolophid (Figure 5AB). The teeth dimensions of larger tapir in Ganxian are comparable to those *M. augustus* from Yenchingkou (Colbert and Hooijer 1953), Bailongdong (Tong et al. 2019), Panxian Dadong (Zhang et al. 1997), Tam Hang South (Bacon et al. 2011), and Mocun Cave (Fan et al. 2022) (Table S7).

Carnivora

Arctonyx collaris: Twenty-four isolated teeth are attributed to *Arctonyx collaris*. Among the upper teeth 18 are complete M1, two fragmentary M1, and among the lower teeth only one complete m1, three fragmentary m1 (Table 4). On the M1, the paracone is the higher cusp (Figure 6A). The three lingual cusps (metaconule, protocone and paraconule) are equal in size, and form a serrated ridge across the occlusal surface. The cingulum is well developed on the lingual side. The m1 is moderately worn, and has well-developed protoconid and metaconid (Figure 6B). The dimensions of the teeth are bigger than those of *Arctonyx collaris* from Juyuan Cave (Wang et al. 2017a), Tham Wiman Nakin (Suraprasit et al. 2021) and within the size range of extant specimens (Colbert and Hooijer 1953) and fossil specimens from Yanlidong (Yao et al. submitted), Duoi U'Oi (Bacon et al. 2008) (Table S8).

Cuon alpinus: Only two teeth (2M1) conform to the dental pattern of the canid *Cuon alpinus*. The paracone of M1 is a large mound, higher than the metacone (Figure 6C). The parastyle is more marked than the metastyle. The Ganxian specimens conform to the dental pattern of the species and range of dimensions of *C. alpinus* identified in Yenchingkou (Colbert and Hooijer 1953), Wuyun Cave (Chen et al. 2002), Duoi U'Oi (Bacon et al. 2008), and Tam Hang South (Bacon et al. 2011) (Table S9).

Neofelis nebulosa: Two isolated teeth of a small felid, one p4 (Figure 6D) and one m1 (Figure 6E-F) have been attributed to *Neofelis nebulosa*. Despite the lack of P4, the most diagnostic tooth to identify the species, the teeth are similar to *N. nebulosa* from Bailongdong and Mocun Cave and the modern species. In relation to dimensions, the Ganxian teeth are similar to those from Bailongdong (Tong et al. 2019) and Mocun Cave (Fan et al. 2022) (Table S10).

Crocuta ultima: The Hyaena is represented by two upper incisors and two lower premolars. I2 has two accessory cusps immediately posterior to the spatula-shaped main cusp (Figure 6G-H). Both p2s have a marked distal accessory cusp but poorly mesial accessory cusp (Figure 6I-J). On the basis of these characteristics, the Ganxian teeth differ from the species (*Pachycrocuta brevirostris*). The morphology and dimensions are similar with the specimens of *C. ultima* from the Middle to Late Pleistocene from Yenchingkou (Colbert and Hooijer 1953), Mocun Cave (Fan et al. 2022), Khok Sung (Suraprasit et al. 2016), and Tham Wiman Nakin (Suraprasit et al. 2021) (Table S11).

Panthera tigris: The *Panthera tigris* are represented by one upper canine, three P3, one P4, one lower incisor (i3), two p4, and three m1. The P4 exhibits one lingual cusp, a worn protocone, and three buccal cusps, a small parastyle and a blade formed by the paracone and the metastyle of equal height (Figure 6K). A deep carnassial notch displays a distinctive fovea between the paracone and the

Figure 5. Perissodactyla from Ganxian Cave. *Rhinoceros sondaicus*: A right DP1 (GX-E3-01) in occlusal view; B right DP2 (29,934) in occlusal view; C right dp1 (29,929) in occlusal view; D left dp2 (29,930) in occlusal view; E left dp3 (GX-E8-02) in occlusal view; F left p3 (31,310) in occlusal view; G right p3 (29,935) in occlusal view; H left p4 (29,933) in occlusal view; I right m1 (30,617) in occlusal view; J left m2 (29,939) in occlusal view; K left m3 (29,932) in occlusal view. *Dicerorhinus sumatrensis*: L right D1 (11,083) in occlusal view; M right P3 (29,937) in occlusal view; N right P3 (29,937) in buccal view; O left M1 (29,938) in occlusal view; P left M1 (29,938) in buccal view; Q left M2 (29,940) in occlusal view; R left M2 (29,940) in buccal view; S right p2 (30,782) in occlusal view; T right m2 (31,308) in occlusal view; U left m3 (31,282) in occlusal view. *Tapirus sinensis*: V right m1 (29,922) in occlusal view. *Megatapirus augustus*: W right M3 (GX-E9-01) in occlusal view; X right p2 (31,533) in occlusal view; Y right p2 (31,533) in lingual view; Z right p4 (GX-E8-01) in occlusal view; AA left m2 (29,924) in lingual view.

metastyle. The m1 consists of two blades separated by a notch (Figure 6O). Its dimensions are clearly in those of *Panthera tigris*. One canine also conforms to this genus. In relation to dimensions, the Ganxian teeth are similar to those from Bailongdong (Tong et al. 2019), Wuyun Cave (Chen et al. 2002), Duoi U'Oi (Bacon et al. 2008), and Tam Hang South (Bacon et al. 2011) (Table S12).

Ursus thibetanus: Forty-eight teeth conform to the dental pattern of *U. thibetanus*. The P4s show sub-triangular outline in occlusal view (Figure 6P). The paracone is larger and higher than the metacone and hypocone. The outline of M1s is sub-rectangular in occlusal view (Figure 6Q). The two buccal cusps (paracone and metacone) are equal in size. The parastyle and the metastyle are well developed. A cingulum is present in the lingual side in six specimens. The M2s are longer than they are wide with a distally elongated talon (Figure 6R). Some teeth display a crenulated cingulum. The m1 is not elongated mesiodistally as *H. malayanus* (Bacon et al. 2018a) (Figure 6S). A deep notch separates the trigonid and talonid. The m2 present in occlusal view a rectangular outline with a distally enlarged talonid (Figure 6T). The dimensions of the teeth show large overlaps with those of *U. thibetanus* from Bailongdong (Tong

Figure 6. Carnivora and Rodentia from Ganxian Cave. *Arctonyx collaris*: A right M1 (30,181) in occlusal view; B right m1 (29,572) in occlusal view. *Cuon alpinus antiquus*: C right M1 (GX-J2-04) in occlusal view. *Neofelis nebulosa*: D right p4 (GX-8) in lingual view; E right m1 (GX-9) in occlusal view; F right m1 (GX-9) in lingual view. *Crocuta ultima*: G right I2 (GX-L4-01) in lingual view; H right I2 (GX-L4-01) in buccal view; I left p2 (GX-7) in occlusal view; J right p2 (30,383) in occlusal view. *Panthera Tigris*: K left P4 (GX-10) in occlusal view; L right i3 (GX-J11-01) in lingual view; M right p4 (GX-K14-01) in occlusal view; N right p4 (GX-K14-01) in buccal view; O right m1 (Gx-11) in occlusal view. *Ursus thibetanus*: P left P4 (31,331) in occlusal view; Q left M1 (29,919) in occlusal view; R right M2 (11,075) in occlusal view; S right m1 (31,036) in occlusal view; T right m2 (11,077) in occlusal view; U left m3 (11,078) in occlusal view. *Ailuropoda baconi* V right P3 (GX-M1-01) in occlusal view; W right P4 (GX-L1-02) in occlusal view; X left M1 (GX-L1-01) in occlusal view; Y left p2 (31,074) in occlusal view; Z left p4 (31,073) in occlusal view; AA left m1 (GX-5) in occlusal view; AB left m1 (GX-5) in buccal view; AC left m2 (GX-6) in occlusal view; AD left m3 (31,110) in occlusal view. *Hystrix subcristata*: AE left m1/2 (GX-13) in buccal view; AF left m1/2 (GX-13) in occlusal view; AG right M1/2 (GX-12) in distal view; AH right M1/2 (GX-12) in occlusal view; AI right I1 (GX-14) in mesial view.

et al. 2019), Yanlidong (Yao et al. submitted), Hualongdong (Tong et al. 2018b), Panxian Dadong (Zhang et al. 1997), Mocun Cave (Fan et al. 2022), Tham Wiman Nakin (Suraprasit et al. 2021), Duoi U'Oi (Bacon et al. 2008), and extant specimens (Suraprasit et al. 2021) (Table S13).

Ailuropoda baconi: Thirty-six isolated giant panda teeth (and teeth fragments) have been recovered at Ganxian Cave. The P3 and P4 both have four cusps, paracone and metacone on the buccal side and protocone and hypocone on the lingual side (Figure 6V-W). The parastyle is well marked. There is a small cusp between the protocone and hypocone. In the P4 there is a cingulum on the lingual aspect (Figure 6W). The outline of M1 is square in occlusal view (Figure 6X). The paracone and the metacone are equal in size. A cingulum on the lingual side is well-developed. The lower p4 presents on the lingual side of the hypoconid an accessory cusplet (entoconid) (Figure 6Z). The m1 displays well-developed accessory cuspids at the buccal side of anterior part (Figure 6AA-AB). The m2 is rectangular in shape in occlusal view (Figure 6AC). The four main cusps (protoconid, metaconid, hypoconid and entoconid) are well-developed. The dimensions of the teeth are larger than the specimens of *Ailuropoda microta* and *Ailuropoda wulingshanensis*, and within the size range of *A. baconi* (Jin et al. 2007; Wang et al. 2017a). We assign these specimens to *A. baconi* (Table S14).

Rodents

Hystrix subcristata: Three hundred and sixty-three isolated teeth, including one hundred and thirty-four incisors, seventy-three premolars, one hundred and fifty-six molars, can be allocated to *Hystrix subcristata* based on their size. The mandibular premolars and molars are straight (Figure 6AE), while the maxillary teeth are curved towards the labial side (Figure 6AG). When the tooth is unworn or lightly, the maxillary tooth presents a deep hypoflexus opening backward in the lingual side and the paraflexus, mesoflexus and metaflexus in the labial side. The hypoflexid opens forward in the labial side in the mandibular tooth. The paraflexid, mesoflexid and metaflexid are in the lingual side (Figure 6AF). When the tooth is heavily worn, the paraflexus, mesoflexus and metaflexus are replaced by three enamel rings (Figure 5AH). The dimensions of the teeth from Ganxian overlap those of *Hystrix subcristata* from Mocun Cave (Fan et al. 2022) (Table S15).

Artiodactyla

Rusa (Cervus) unicolour: 484 permanent premolars and molars and 32 deciduous teeth, belonging to a large-sized cervid are referred to *Cervus unicolour* (Table 5). The P2 has two distinct lobes on the lingual size with a clear separation between the protocone and hypocone (Figure 7D). The paracone rib is prominent. The metastyle is more developed than the parastyle. The outline of P3 is square in occlusal view (Figure 7E). The morphology of the P3 is similar to that of the P2. The metastyle of P3 is less developed than in P2. The P4 is rectangle in occlusal view and has a small groove between the two lingual cusps (Figure 7F). The metastyle is less developed than P2 and P3. Some P4 present a developed cingulum on the lingual side. The upper molars present entostyles on the lingual side (Figure 7G-I). The p3s are not molarized (Figure 7K), and some p4 show a low degree of molarisation or incomplete molarisation (Figure 7L). The dimensions of the Ganxian teeth show large overlaps with those of *Rusa (Cervus) unicolour* from Longgudong, Bailongdong (Tong et al. 2019), Yanlidong (Yao et al. submitted), Tham Wiman Nakin Caves (Suraprasit et al. 2021), Tam Hang South (Bacon et al. 2011), Mocun Cave (Fan et al. 2022), Duoi U'Oi (Bacon et al. 2008), and extant specimens (Suraprasit et al. 2021) (Table S16).

Muntiacus muntjak: The small-sized cervid (*Muntiacus muntjak*) is represented by 397 specimens. The P2 displays a salient metastyle and paracone rib (Figure 7Q). The protocone and hypocone are separated by a deep groove. The P3 has a less-marked groove between the two lingual cusps (Figure 7R). The metastyle and paracone rib are less-developed than the P2. On the P4, the groove between protocone and hypocone is sometimes absent (Figure 7S). The protocone and the hypocone are equal in size. The upper molars have developed mesostyle and metacone, and show an entostyle (Figure 7T-V). One p4 displays a molarisation. The dimensions of Ganxian teeth overlap largely with those of *M. muntjak* from Yanlidong (Yao et al. submitted), Tam Hang South (Bacon et al. 2011), Mocun Cave (Fan et al. 2022), Duoi U'Oi (Bacon et al. 2008), and extant specimens (Suraprasit et al. 2021) (Table S17).

Muntiacus reevesi: Twenty-nine teeth are assigned to *Muntiacus reevesi*. The P2 has a prominent the metastyle and the paracone rib. The protocone and hypocone are separated by a groove. The groove is less-marked or absent in P3 and P4. There is the trace of cingulum on the lingual side in some specimens. The upper molars have a weak entostyle (Figure 7AC-AE). The morphology conforms of *M. reevesi* from Bailongdong (Tong et al. 2019), Mocun Cave (Fan et al. 2022), Yangjiawan and Fuyan Caves (Zhang et al. 2018). The dimensions of Ganxian teeth falls within the range of fossil specimens from Bailongdong (Tong et al. 2019), Mocun Cave (Fan et al. 2022), Yangjiawan and Fuyan Caves (Zhang et al. 2018) and extant specimens (Suraprasit et al. 2021) (Table S18). Based on their extremely small size, we assigned these specimens to *M. reevesi*.

Bos gaurus: Twenty-seven permanent teeth are identified as belonging to *Bos gaurus*. The occlusal outline of M1 is sub-square and that of M2 is rectangular (Figure 8B-C). On M1 and M2 moderately worn, the entostyles are generally bifurcated or sometimes trifurcated (Figure 8B-C). The M3 exhibits a well-developed metastyle projecting more distally (Figure 8D). The entostyle on the M3 is not bifurcated. The p3 and p4 show a larger metaconid and a buccolingual constriction of the external postprotocristid (Figure 8 E and C). A deep distal valley can be observed in lingual side on p3 and p4 (Figure 8 F and H). Lower molars generally possess a weak metastylid compared to *Bubalus arnee* (Figure 8I, K and M). There is vertical groove along the lingual surface of columns in buccal view (Figure 8J, L and N). The m3 presents a prominent posterior entostylid (Figure 8M-N). The dimensions of the teeth are comparable to those from Bailongdong (Tong et al. 2019), Khok Sung (Suraprasit et al. 2016), Tham Wiman Nakin (Suraprasit et al. 2021) and extant specimens (Table S19). Based on their larger sizes (than *Bos javanicus* and *Bos sauveli*), more developed metaconids and more mesiodistally constricted postprotocristids on the p3 and p4, we attributed these specimens to *B. gaurus*.

Bubalus arnee: Sixteen isolated teeth are attributed to *Bubalus arnee*. The incomplete DP2 is elongated, with a prominent paracone and metastyle. The P3 has a subtriangular outline, characterised by a distinct parastyle, paracone rib, and metastyle and a U-shaped fossette (Figure 8O). The p2 displays a well-developed postentocristid and posthypocristid (Figure 8Q-R). A well-developed preprotoconulidcristid is present on p3 (Figure 8S-T). On the p4, the postprotocristid is anteroposteriorly constricted, and fuses with the posthypocristid beyond the middle stage of wear (Figure 8U-V). A well-developed metastylid is present on lower molar (Figure 8 W and Y). The posterior ectostylid is absent on the m3 (Figure 8Z). The dimensions of all the Ganxian teeth are comparable to those of specimens from Khok Sung (Suraprasit

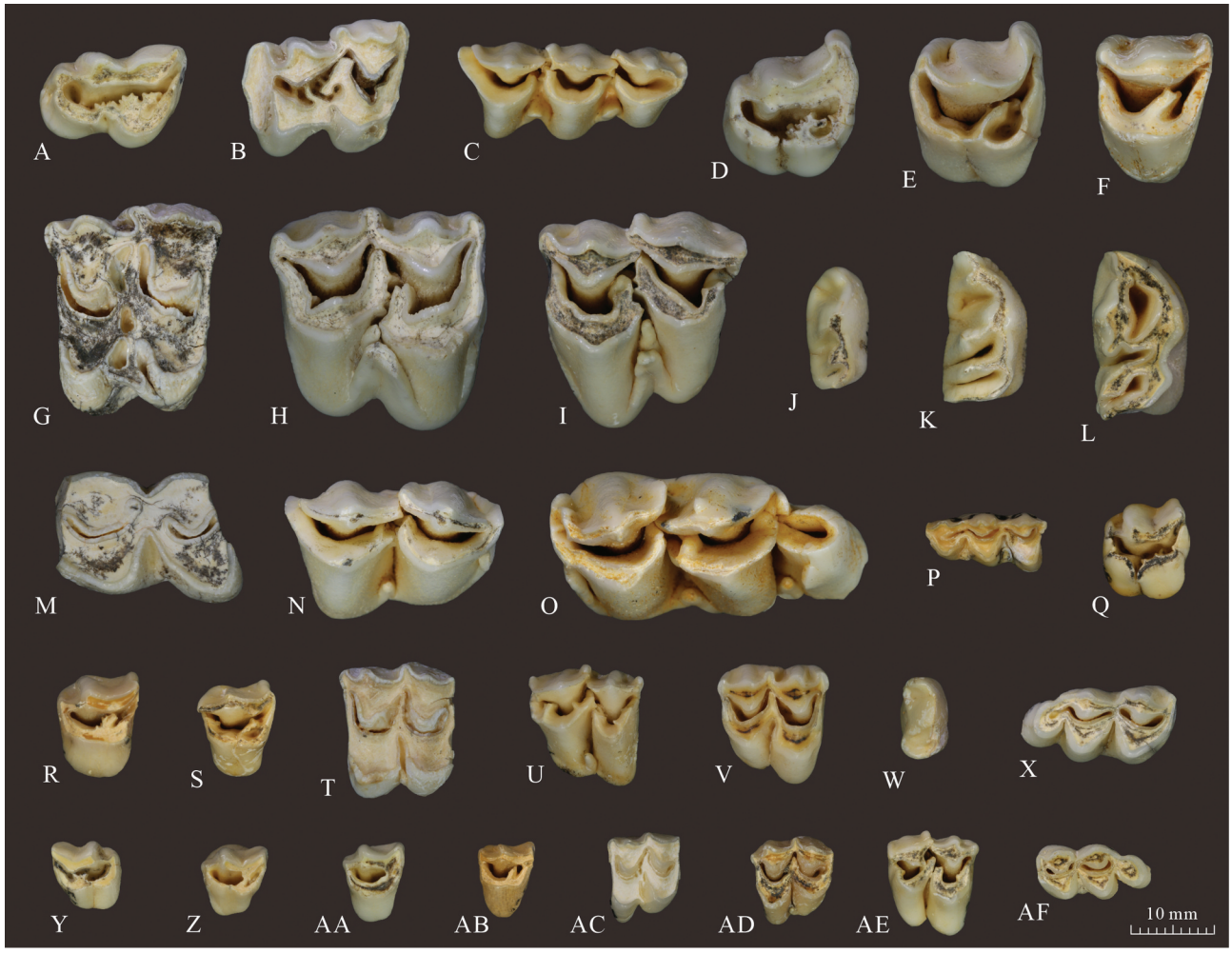

Figure 7. Fossil teeth of *Rusa unicolour* (A-O), *Muntiacus muntjak* (P-X), and *Muntiacus reevesi* (Y-AF) from Ganxian Cave. A left DP2 (31,479) in occlusal view; B left DP3 (30,346) in occlusal view; C right dp4 (30,930) in occlusal view; D left P2 (30,462) in occlusal view; E left P3 (31,473) in occlusal view; F left P4 (30,088) in occlusal view; G left M1 (30,818) in occlusal view; H right M2 (31,262) in occlusal view; I left M3 (31,414) in occlusal view; J right p2 (31,170) in occlusal view; K right p3 (31,476) in occlusal view; L right p4 (31,080) in occlusal view; M left m1 (31,481) in occlusal view; N right m2 (30,628) in occlusal view; O left m3 (30,866) in occlusal view. P right dp4 (30,016) in occlusal view; Q left P2 (31,158) in occlusal view; R left P3 (29,463) in occlusal view; S left P4 (30,912) in occlusal view. T left M1 (30,494) in occlusal view; U right M2 (29,456) in occlusal view; V right M3 (29,458) in occlusal view; W right p2 (30,431) in occlusal view; X right m3 (31,384) in occlusal view; Y right P2 (31,127) in occlusal view; Z left P2 (31,440) in occlusal view; AA left P3 (31,101) in occlusal view; AB left P4 (29,755) in occlusal view; AC left M1 (30,018) in occlusal view; AD left M2 (31,164) in occlusal view; AE right M3 (31,160) in occlusal view; AF left m3 (31,126) in occlusal view.

et al. 2016) and Tham Wiman Nakin (Suraprasit et al. 2021) assigned to *Bubalus arnee* (Table S20).

Megalovis guangxiensis: Four teeth (one p4, two m2s and one m3) are attributed to *Megalovis guangxiensis*. The p4 is molarized and has a smaller distal lobe than mesial lobe (Figure 8AA). The protoconid and metaconid are developed (Figure 8AB-AC). The m2s have a sub-triangular occlusal outline for mesial and distal lobes (Figure 8AD). A prominent ectostylid is present between the protoconid and hypoconid (Figure 8AE). The m3 has four main cusps and a more or less developed hypoconulid (Figure 8AG). In the m3, the ectostylid is weak between the protoconid and hypoconid, but no posterior ectostylid between the hypoconid and hypoconulid (Figure 8AH). The p4 and m2 of Ganxian are larger than those of Longgupo (Huang and Fang 1991), Sanhe Cave (Dong et al. 2011), and Daxin Hei Cave (Han 1982), fall with the range of specimens from *Gigantopithecus* Cave (Han 1987) and Queque Cave (Dong et al. 2020). The length of m3 exceed the known ranges of fossil *Megalovis guangxiensis* (Han 1982, Han 1987; Huang and Fang 1991; Dong et al. 2011, 2020) (Table S21).

Capricornis sumatraensis: The P4 is subtriangular in shape and presents a well-developed parastyle and metastyle (Figure 8AJ). From the occlusal aspect, upper molars display a subtriangular-shaped mesial lobe and a pentagonal-shaped distal lobe (Figure 8AK-AL). The mesostyle on upper molars is often more pronounced than the parastyle. On moderately worn m3, the back fossette on the third lobe is absent. The dimensions of the teeth are comparable to *C. sumatraensis* from Tham Wiman Nakin (Suraprasit et al. 2021), Tham Prakai Phet (Wattanapituksakul 2016), Tam Hang South (Bacon et al. 2011), Duoi U'Oi (Bacon et al. 2008), and extant specimens (Wattanapituksakul et al. 2018) (Table S22).

Sus scrofa: Five hundred and twenty-one isolated teeth, including 51 incisor, 12 canines, 449 cheek teeth, 9 milk teeth, are attributed to the larger pig *Sus scrofa*. One maxilla with P3/P4/M1 is also recorded. All these elements resemble those of modern *Sus scrofa*: smooth enamel, and numerous accessory tubercles with characteristic star-like folds on molars (Figure 9). The identifiable lower canines present the typical

Figure 8. Fossil teeth of *Bos gaurus* (A-N), *Bubalus arnee* (O-Z), *Megalovis guangxiensis* (AA-AI), and *Capricornis sumatraensis* (AJ-AM) from Ganxian Cave. A left P4 (GX-L1-47) in occlusal view; B right M1 (30,937) in occlusal view; C left M2 (GX-E8-4) in occlusal view; D right M3 (GX-E8-03) in occlusal view; E left p3 (30,927) in occlusal view; F left p3 (30,927) in lingual view; G left p4 (GX-E8-08) in occlusal view; H left p4 (GX-E8-08) in lingual view; I left m1 (GX-E7-05) in occlusal view; J left m1 (GX-E7-05) in buccal view; K right m2 (11,098) in occlusal view; L right m2 (11,098) in buccal view; M right m3 (29,760) in occlusal view; N right m3 (29,760) in buccal view; O left P3 (GX-E7-06) in occlusal view; P right P4 (GX-E8-12) in occlusal view; Q right p2 (30,090) in occlusal view; R left p2 (GX-19) in occlusal view; S right p4 (GX-E8-10) in occlusal view; T right p4 (GX-E8-10) in lingual view; U left p4 (31,359) in occlusal view; V left p4 (31,359) in lingual view; W right m2 (GX-E7-03) in occlusal view; X right m2 (GX-E7-03) in buccal view; Y left m3 (GX-E5-01) in occlusal view; Z left m3 (GX-E5-01) in buccal view; AA left p4 (31,358) in occlusal view; AB left p4 (31,358) in buccal view; AC left p4 (31,358) in lingual view; AD left m2 (29,906) in occlusal view; AE left m2 (29,906) in buccal view; AF left m2 (29,906) in lingual view; AG left m3 (30,239) in occlusal view; AH left m3 (30,239) in buccal view; AI left m3 (30,239) in lingual view; AJ right P4 (31,209) in occlusal view; AK left M2 (31,312) in occlusal view; AL left M3 (29,898) in occlusal view; AM right m3 (30,376) in buccal view.

Figure 9. Fossil teeth of *Sus scrofa* (A-P) and *Sus xiaozhu* (Q-S) from Ganxian Cave. A left i2 (29,894) in lingual view; B left C (GX-15) in buccal view; C and D left c (31,044); E right P2 (30,980) in occlusal view; F right P3 (30,951) in occlusal view; G left P4 (29,857) in occlusal view; H left M1 (30,510) in occlusal view; I right M2 (31,135) in occlusal view; J left M3 (29,746) in occlusal view; K left p2 (30,957) in occlusal view; L right p3 (30,386) in occlusal view; M right p4 (31,020) in occlusal view; N right m1 (29,851) in occlusal view; O left m2 (29,810) in occlusal view; P right m3 (30,863) in occlusal view; Q right M2 (29,869) in occlusal view; R right M2 (31,526) in occlusal view; S right m2 (30,861) in occlusal view.

'scrofic' type, with a triangular cross-section, a high-crown, a thin enamel, and with a lingual side wider than the buccal (Figure 9C-D). The dimensions of the Ganxian teeth show large overlap with those of *S. scrofa* from Bailongdong (Tong et al. 2019), Duoi U'Oi (Bacon et al. 2008), Tam Hang South (Bacon et al. 2011), Tham Wiman Nakin (Suraprasit et al. 2021), and Mocun Cave (Fan et al. 2022) (Table S23).

Sus xiaozhu: The *Sus xiaozhu* is documented by 12 permanent molars teeth. The M1 has a rectangular in outline with four main cusps (Figure 9Q). These cusps are almost equal in size. The morphology of the M2 is similar to that of the M1 (Figure 9R). The M2 has more developed anterior cingulum and pentapreconule. A small accessory cuspids is present in the lingual valley. The m2 crown displays a rectangular outline (Figure 9S). The m2 have four main cusps of the same size (protoconid, metaconid, hypoconid and entoconid). There is no accessory cuspid in the valley. The dimensions of the teeth show large overlap with those of *S. xiaozhu* from Longgupo (Huang and Fang 1991), Mohui Cave (Wang 2005), Longgudong (Zheng 2004), Bijiashan (Han et al. 1975), Dongpaoshan (Wang et al. 1982), and *Gigantopithecus* Cave (Han 1987). Based on their extremely small size, we attributed these teeth to *S. xiaozhu* (Table S24).

Discussion

Biochronological framework of Ganxian cave

The newly recovered Ganxian mammalian assemblage is composed of 28 identified taxa belonging to six orders (Primates, Carnivora, Proboscidea, Perissodactyla, Artiodactyla, and Rodentia). The Ganxian fauna is composed of eight extinct species (*Pongo weidenreichi, Ailuropoda baconi, Stegodon orientalis, Tapirus sinensis, Megatapirus augustus, Crocuta ultima, Megalovis guangxiensis, and Sus xiaozhu*) and a larger portion of modern species. The Ganxian faunal composition has all the characteristics of a late Middle Pleistocene mammalian assemblage with biochronological age estimates in agreement with age estimates obtained using

U-series dating, coupled ESR/U-series dating, and magnetostratigraphic dating methods.

No archaic elements which are characteristic of the Early Pleistocene '*Gigantopithecus-Sinomastodon* fauna', such as *Ailuropoda microta, Stegodon huananensis, Sinomastodon, Hesperotherium, Tapirus sanyuanensis. Gigantopithecus blacki*, were recovered in the Ganxian assemblage. Thus, the Ganxian fauna is distinctly different from the Early Pleistocene *Gigantopithecus* fauna (Chow 1957; Wang et al. 2007; Jin et al. 2014) (Figure 10).

Ganxian fauna resembles faunas of approximately the same age, Daxin Hei Cave (Han 1982) and Hejiang Cave (Zhang et al. 2014), and the slightly older Bailongdong (Tong et al. 2019), Bulalishan (Zhang et al. 1973), Yanlidong (Yao et al. submitted), and Tham Khuyen (Schwartz et al. 1994). However, Ganxian is devoid of archaic components found to be present on those sites, such as *Pachycrocuta sinensis* at Bailongdong (Tong et al. 2019), *G. blacki* at Bulalishan (Zhang et al. 1973), Daxin Hei Cave (Han 1982), and Tham Khuyen (Schwartz et al. 1994), and *Sus peii* at Yanlidong (Yao et al. submitted).

The resemblance of the Ganxian fauna to those of coeval localities such as Wuyun Cave (Chen et al. 2002), Hualongdong (Tong et al. 2018a) and Panxian Dadong (Si et al. 1993; Zhang et al. 1997) in China, Khok Sung (Suraprasit et al. 2016) and Tham Wiman Nakin (Suraprasit et al. 2021) in Thailand is striking. Indeed, they are composed of archaic species typical of the '*Stegodon-Ailuropoda* ' faunas and modern species still living in Asia.

Ganxian fauna has *A. baconi, S. orientalis*, and *E. maximus*, so it is distinctly different from those Late Pleistocene faunas, such as Zhiren Cave (Jin et al. 2009), Luna Cave (Bae et al. 2014), Tam Hang South (Bacon et al. 2011), Nam Lot (Bacon et al. 2018b), and Mocun Cave (Fan et al. 2022).

Furthermore, the Ganxian fauna is distinguished by its relative modernity, whereas those of Duoi U'Oi (Bacon et al. 2008)

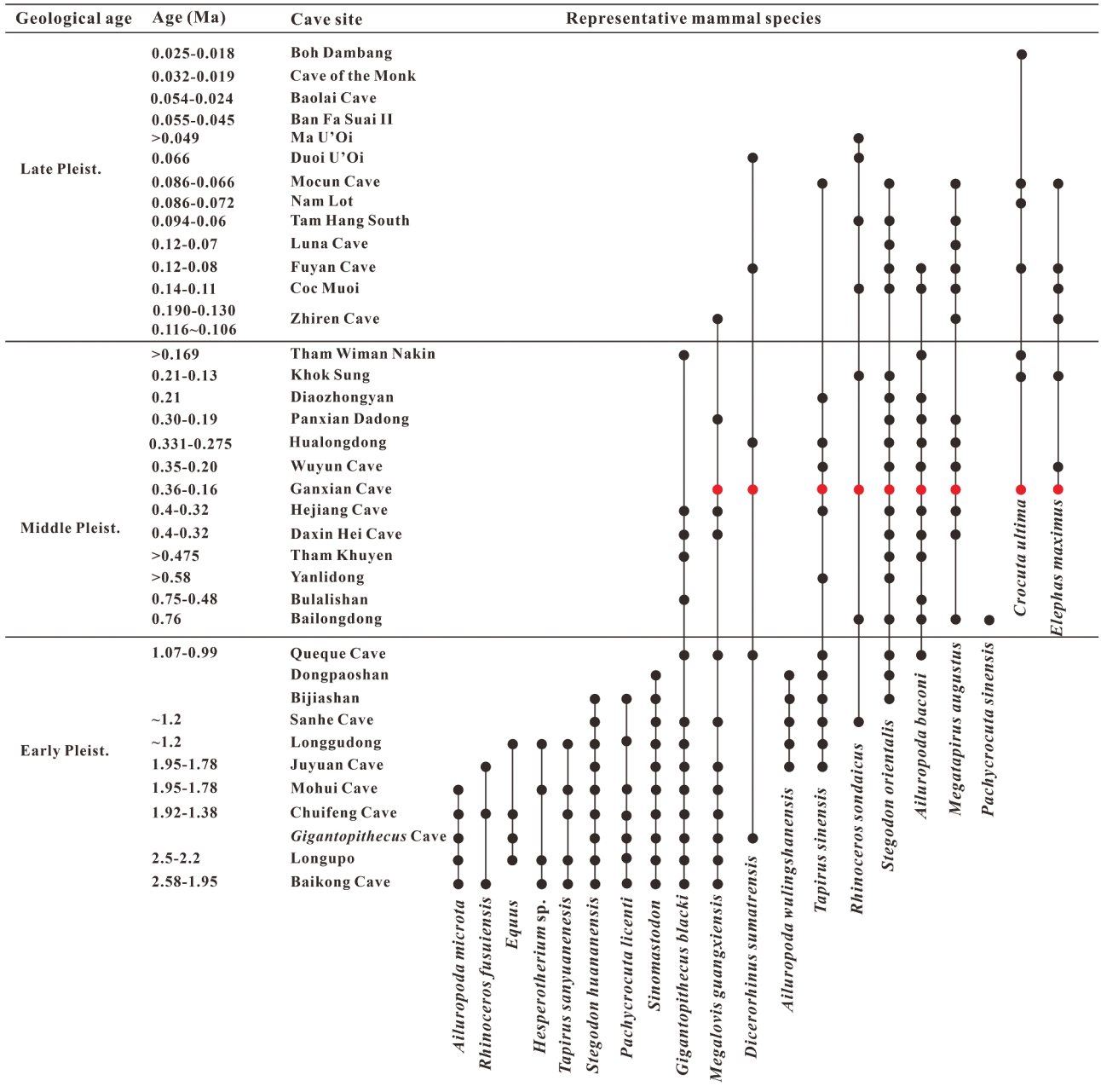

Figure 10. Biochronological framework designed with the thirty- seven well-documented faunas from the Indochinese province. Abbreviations: Pleist. = Pleistocene.

and Ma U'Oi (Bacon et al. 2004, 2006) in northern Vietnam (respectively 66 ± 3 ka and >47 ± 4 ka) are totally modern in their composition.

Although the chronological significance of *Elephas* is an unresolved issue (Zeitoun et al. 2015, 2016), the *E. maximus* fossils of the Ganxian Cave may represent the earliest appearance of *E. maximus* in mainland southeast Asia and south China. Compared with the fossil sites with the occurrences of *E. maximus*, such as Coc Muoi (Bacon et al. 2018a) in Vietnam, and Wuyun Cave (Chen et al. 2002), Panxian Dadong (Si et al. 1993; Zhang et al. 1997), Fuyan Cave (Li et al. 2013), Mawokou (Wang et al. 2017b), Yangjiawa (Tong et al. 2018a) in South China, the Ganxian Cave site, which is dated to between 168.9 ± 2.4 ka and 362 ± 78 ka based on U-series and coupled ESR/U-series dating methods, may be the site of the earliest appearance of *E. maximus*. Of course, this is just a throw-away conclusion for now, more fossils with precise absolute age constrains are the key to solving first appearance of *E. maximus* in mainland Southeast Asia and south China.

Paleoenvironmental implications

Extant orangutans (*Pongo pygmaeus, Pongo abelii*, and *Pongo tapanuliensis*) are the most arboreal of the great apes and are representative members of evergreen tropical rain forest communities (MacKinnon 1974; Davies 1986; Payne and Prudente 2008; Nater et al. 2017). As such, in palaeontological reconstructions of paleoenvironments, the presence of orangutan specimens in fossil assemblages often indicates the existence of a forested habitat (Van den Bergh et al. 2001; Storm et al. 2005; Tougard and Montuire 2006). This is consistent with the $\delta^{13}C$ results obtained for specimens from several Pleistocene cave sites in southern China, such as Yanliang, Liucheng, Mohui, Sanhe, Tantang, Baxian and Quzai Caves (Wang et al. 2007; Nelson 2014; Qu et al. 2014; Li et al. 2017; Ma et al. 2017; Stacklyn et al. 2017, 2019). *U. thibetanus* prefers moist deciduous forests, bushy areas, hills and mountains (Nowak 1999). *C. ultima* was a predator that probably feed C_4-plant consumers, as demonstrated by carbon isotopic results from the late Middle Pleistocene site of Tham Wiman Nakin (Pushkina et al. 2010). The presence of the *P. tigris* at the Ganxian Cave site indicates the presence of a diversified habitat with closed forests and zones with more open forests (Schaller 1967).

The Ganxian fauna is characterised by the coexistence of *R. sondaicus* and *D. sumatrensis*, which suggests humid condition. The Javan rhino inhabits tall grass and lowland reed beds in tropical rain forests with a good supply of water and plentiful mud wallows. *R. sondaicus* is an exclusive browser feeding on shoots, twigs, young foliage and fruits (Nowak 1999). The Sumatran rhino is found in a wide variety of habitats, including lowland rain forests and swamps to mountain moss forests, but always near water and salt licks. *D. sumatrensis* is a browser, feeding on leaves, twigs and fruits (Nowak 1999).

In summary, the Ganxian fauna assemblage suggests that between 168.9 ± 2.4 ka and 362 ± 78 ka, the environment was characterised by a forest and some open habitats, under warm and humid conditions. At latitudes close to that of Ganxian Cave (23°N), sedimentological and palynological records of the Leizhou Peninsula (20°-21°N) in southern China show that a slightly drier and cooler condition in MIS 10 was followed by a wetter and warmer climate in MIS 9. The montane forest reached down to the lowland by at least 600 m during the MIS 6 and 8 in a cool and relatively wet condition (Zheng and Lei 1999). This palynological evidence from the Leizhou Peninsula supports our paleoenvironment reconstructions of the mammalian fauna.

Conclusion

The fauna consists of 28 large mammalian species, and is characterised by the combination of *Macaca* sp., *Trachypithecus/Presbytis* sp., *Hylobates* sp., *Pongo weidenreichi, Elephas maximus, Stegodon orientalis, Rhinoceros* sp., *Rhinoceros sondaicus, Dicerorhinus sumatrensis, Tapirus sinensis, Megatapirus augustus, Arctonyx collaris, Cuon alpinus, Neofelis nebulosa, Crocuta ultima, Panthera tigris, Ursus thibetanus, Ailuropoda baconi, Hystrix subcristata, Rusa (Cervus) unicolour, Muntiacus muntjak, Muntiacus reevesi, Bos gaurus, Bubalus arnee, Megalovis guangxiensis, Capricornis sumatraensis, Sus scrofa, Sus xiaozhu*, showing the features of typical *Ailuropoda-Stegodon* fauna. The arising of *E. maximus* in Ganxian may probably represent the earliest appearance of Asian elephant. The palaeoenvironmental reconstruction based on the study of the Ganxian faunal assemblage suggests a forested and some open habitats, within warm and humid conditions.

Acknowledgments

We thank Q. Y. Huang, and F. Tian (Tiandong County Museum), C. L. Huang and S. W. Xie (Natural History Museum of Guangxi), J. P. Li (Anthropology Museum of Guangxi), for their participation in the field investigation and excavation.

Disclosure statement

No potential conflict of interest was reported by the authors.

Funding

This study was supported by the Major Program of National Social Science Foundation of China (20&ZD246); the National Natural Science Foundation of China 41877430,42002025 (42002025, 41877430); the BaGui Scholars Project of the Guangxi Zhuang Autonomous Region.

References

Bacon AM, Antoine PO, Nguyen TMH, Westaway K, Tuan NA, Duringer P, Zhao J, Ponche JL, Dung SC, Nghia TH, et al. 2018a. A rhinocerotid-dominated megafauna at the MIS6-5 transition: the late middle pleistocene coc muoi assemblage, Lang Son province. Vietnam Quat Sci Rev. 186:123–141. doi:10.1016/j.quascirev.2018.02.017.

Bacon AM, Bourgon N, Dufour E, Zanolli C, Duringer P, Ponche J-L, Antoine P-O, Shackelford L, Nguyen Thi Mai H, Sayavonkhamdy T, et al. 2018b. Nam Lot (MIS 5) and Duoi U'Oi (MIS 4) Southeast Asian sites revisited: zooarchaeological and isotopic evidences. Paleogeogr Paleoclimatol Paleoecol. 512:132–144. doi:10.1016/j.palaeo.2018.03.034.

Bacon AM, Demeter F, Duringer R, Helm C, Bano M, Long VT, Thuy NTK, Antoine PO, Mai BT, Huong NTM, et al. 2008. The Late Pleistocene Duoi U'Oi cave in northern Vietnam: palaeontology, sedimentology, taphonomy and palaeoenvironments. Quat Sci Rev. 27(15–16):1627–1654. doi:10.1016/j.quascirev.2008.04.017

Bacon AM, Demeter F, Rousse S, Long VT, Duringer P, Antoine PO, Thuy NK, Mai BT, Huong NTM, Dodo Y, et al. 2006. New palaeontological assemblage, sedimentological and chronological data from the Pleistocene Ma U'Oi cave (northern Vietnam). Paleogeogr Paleoclimatol Paleoecol. 23(3–4):280–298. doi:10.1016/j.palaeo.2005.07.023

Bacon AM, Demeter F, Schuster M, Long VT, Thuy NK, Antoine PO, Sen S, Nga HH, Huong NM. 2004. The Pleistocene Ma U'Oi cave, northern Vietnam: palaeontology, sedimentology and palaeoenvironments. Geobios. 37(3):305–314. doi:10.1016/j.geobios.2003.03.010.

Bacon AM, Duringer P, Antoine PO, Demeter F, Shackelford L, Sayavongkhamdy T, Sichanthongtip P, Khamdalavong P, Nokhamaomphu S, Sysuphanh V, et al. 2011. The Middle Pleistocene mammalian fauna from Tam Hang karstic deposit, northern Laos: new data and evolutionary hypothesis. Quat Int. 245(2):315–332. doi:10.1016/j.quaint.2010.11.024

Bacon AM, Duringer P, Westaway K, Joannes-Boyau R, Zhao J, Bourgon N, Dufour E, Pheng S, Tep S, Ponche JL, et al. 2018c. Testing the Savannah corridor hypothesis during MIS2: the Boh

Dambang hyena site in southern Cambodia. Quat Int. 464:417–439. doi:10.1016/j.quaint.2017.10.047.
Bae CJ, Wang W, Zhao J, Huang S, Tian F, Shen G. 2014. Modern human teeth from Late Pleistocene Luna Cave (Guangxi, China). Quat Int. 354:169–183. doi:10.1016/j.quaint.2014.06.051.
Cai Y, Qiang X, Wang X, Jin C, Wang Y, Zhang Y, Trinkaus E, An Z. 2017. The age of human remains and associated fauna from Zhiren Cave in Guangxi, southern China. Quat Int. 434:84–91. doi:10.1016/j.quaint.2015.12.088.
Chen G, Wang W, Mo J, Huang Z, Tian F, Huang W. 2002. Pleistocene vertebrate fauna from Wuyun cave of Tiandong county, Guangxi. Vertebr Palasiat. 40: 42–51. [in Chinese with English summary].
Chow MC. 1957. Characteristic and correlation of the Tertiary and early Quaternary mammalian faunas from southern China. Chin Sci Bull. 13:394–399.
Ciochon R, Long VT, Larick R, González L, Grün R, de VJ, Yonge C, Taylor L, Yoshida H, Reagan M. 1996. Dated co-occurrence of *Homo erectus* and *Gigantopithecus* from Tham Khuyen cave. Vietnam Proc Natl Acad Sci. 93 (7):3016–3020. doi:10.1073/pnas.93.7.3016.
Colbert EH. 1943. Pleistocene vertebrates collected in Burma by the American Southeast Asiatic expedition. In: de Terra H, Movius HL, Colbert EH, Bequaert J, editors. Research on early man in burma, with supplementary reports upon the pleistocene vertebrates and mollusks of the region, and pleistocene geology and early man in java. Trans Am Phil Soc. 32:395–429.
Colbert EH, Hooijer DA. 1953. Pleistocene mammals from the limestone fissures of Szechwan, China. Bull Amer Mus Nat Hist. 102:1–134.
Davies G. 1986. The orang-utan in Sabah. Oryx. 20(1):40–45. doi:10.1017/S0030605300025904.
de Terra H. 1938. Preliminary report on recent geological and archaeological discoveries relating to early man in Southeast Asia. Proc Natl Acad Sci. 24 (10):407–413. doi:10.1073/pnas.24.10.407.
Dong W, Pan W, Sun C, Xu Q, Qin D, Wang Y. 2011. early pleistocene ruminants from the sanhe cave, Chongzuo, Guangxi, South China. Acta Anthropol Sinica. 30(2):192–205. [in Chinese with English summary].
Dong W, Wang Y, Bai W, Zhang Y, Liu J, Jin C. 2020. Late early pleistocene artiodactyls associated with *Gigantopithecus* from Queque Cave, Chongzuo, Guangxi, South China. Acta Anthropol Sinica. 39: 306–318. [in Chinese with English summary].
Duval M, Fang F, Suraprasit K, Jaeger JJ, Benammi M, Chaimanee Y, Cibanal JI, Grün R. 2019. Direct ESR dating of the Pleistocene vertebrate assemblage from Khok Sung locality, Nakhon Ratchasima province, Northeast Thailand. Palaeontol Electron. 22:1–25.
Esposito M, Chaimanee Y, Jaeger J, Reyss J. 1998. Datation des concrétions carbonatées de la ≪ Grotte du Serpent ≫ (Thaïlande) par la méthode Th/U. Comptes Rendus Acad Sci - Ser IIA Earth Planet Sci. 326(9):603–608. doi:10.1016/S1251-8050(98)80250-4.
Esposito M, Reyss J, Chaimanee Y, Jaeger J. 2002. U-series dating of fossil teeth and carbonates from Snake Cave, Thailand. J Archaeol Sci. 29:341–349. doi:10.1006/jasc.2002.0718.
Fan Y, Shao Q, Bacon AM, Liao W, Wang W. 2022. Late Pleistocene large-bodied mammalian fauna from Mocun cave in south China: palaeontological, chronological and biogeographical implications. Quat Sci Rev. 294:107741. doi:10.1016/j.quascirev.2022.107741.
Filoux A, Wattanapituksakul A. 2019. The Late Pleistocene Orangutan from Tham Prakai Phet: New discoveries. Ann Paleontol. 105: 287–293. doi:10.1016/j.annpal.2019.03.004
Ge JY, Deng C, Wang Y, Shao Q, Zhou X, Xing S, Pang H, Jin C. 2020. Climate-influenced cave deposition and human occupation during the Pleistocene in Zhiren Cave, southwest China. Quat Int. 559:14–23. doi:10.1016/j.quaint.2020.01.018.
Han D. 1982. Mammalian fossils from Tahsin county, Guangxi. Vertebr Palasiat. 20: 59–64. [in Chinese with English summary].
Han D. 1982. Mammalian fossils from Tahsin County, Guangxi. Vertebr Palasiat 20:58–64. [in Chinese with English summary].
Han D. 1987. Artiodactyla fossils from Liucheng *Gigantopithecus* cave in Guangxi. Memoirs of the Institute of Vertebrate Palaeontology and Palaeoanthropology, Academia Sinica 18. Beijing: Science Press; p. 135–208.
Han F, Bahain JJ, Deng C, É B, Hou Y, Wei G, Huang W, Garcia T, Shao Q, He C, et al. 2017. The earliest evidence of hominid settlement in China: combined electron spin resonance and uranium series (ESR/U-series) dating of mammalian fossil teeth from Longgupo cave. Quat Int. 434:75–83. doi:10.1016/j.quaint.2015.02.025.
Han F, Shao Q, Bahain -J-J, Sun X, Yin G. 2019. Coupled ESR and U-series dating of Middle Pleistocene hominin site Bailongdong cave, China. Quat Geochronol. 49:291–296. doi:10.1016/j.quageo.2018.02.004.
Han D, Xu CH. 1985. Pleistocene mammalian faunas of China. In: Rukang W, Olsen JW, editors. Palaeoanthropology and Palaeolithic Archaeology in the People's Republic of China. New York: Academic Press; p. 267–286.
Han D, Xu C, Yi G. 1975. Quaternary mammal fossils from Bijiashan, Liuzhou, Guangxi. Vertebr Palasiat. 13: 250–256. [in Chinese with English summary].
Huang W. 1979. On the age of the cave faunas of South China. Vertebr Palasiat. 17: 342–343. [in Chinese with English summary].
Huang W, Fang Q. 1991. Wushan Hominid Site. Beijing: China Ocean Press.
Hu C, Qi T. 1978. Gongwangling Pleistocene mammalian fauna of Lantian, Shaanxi. Beijing: Science Press.
Jiangzuo QG, Liu JY, Wagner J, Chen J. 2018a. Taxonomical revision of "*Arctonyx*" fossil remains from the Liucheng *Gigantopithecus* Cave (South China) by means of morphotype and morphometrics, and a review of Late Pliocene and Early Pleistocene *Meles* fossil records in China. Palaeoworld. 27 (2):282–300. doi:10.1016/j.palwor.2017.12.001.
Jiangzuo QG, Liu JY, Wagner J, Dong W, Chen J. 2018b. Taxonomical revision of fossil *Canis* in Middle Pleistocene sites of Zhoukoudian, Beijing, China and a review of fossil records of *Canis mosbachensis variabilis* in China. Quat Int. 482:93–108. doi:10.1016/j.quaint.2018.04.003.
Jin CZ, Ciochon RL, Dong W, Hunt RM, Liu JY, Jaeger M, Zhu QZ. 2007. The first skull of the earliest giant panda. Proc Nat Acad Sci. 104 (26):10932–10937. doi:10.1073/pnas.0704198104.
Jin C, Pan W, Zhang Y, Cai Y, Xu Q, Tang Z, Wang W, Wang Y, Liu J, Qin D, et al. 2009. The *Homo sapiens* Cave hominin site of Mulan Mountain, Jiangzhou District, Chongzuo, Guangxi with emphasis on its age. Chin Sci Bull. 54(21):3848–3856. doi:10.1007/s11434-009-0641-1
Jin C, Wang Y, Deng C, Harrison T, Qin D, Pan W, Zhang Y, Zhu M, Yan Y. 2014. Chronological sequence of the early Pleistocene *Gigantopithecus* faunas from cave sites in the Chongzuo, Zuojiang River area, South China. Quat Int. 354:4–14. doi:10.1016/j.quaint.2013.12.051.
Jin C, Zheng J, Wang Y, Xu Q. 2008. The stratigraphic distribution and zoogeography of the Early Pleistocene mammalian fauna from South China. Acta Anthropol Sinica. 27(4):304–317. [in Chinese with English summary].
Kahlke HD, Hu C. 1961. On the complex of the *Stegodon-Ailuropoda*-fauna of southern China and the chronological position of *Gigantopithecus blacki* V. Koenigswald Vertebr Palasiat. 2:3–28.
Liang H, Harrison T, Shao QF, Bahain JJ, Zhao JX, Bae CJ, Liao W, Wang W. submitted. New Middle Pleistocene *Pongo* fossils from Ganxian Cave in southern China with implications for understanding the dental size evolution in *Pongo*. JHum Evol.
Liang H, Liao W, Yao Y, Bae CJ, Wang W. 2020. A late Middle Pleistocene mammalian fauna recovered in northeast Guangxi, southern China: implications for regional biogeography. Quat Int. 563:29–37. doi:10.1016/j.quaint.2019.12.013.
Liao W, Feng YX, Zhao JX, Jiang TY, Yao YY, Liang H, Nguyen AD, Bae CJ, Wang W. 2020. Combined U-series dating of cave pearls and mammal fossils: constraint on the age of a late middle pleistocene *Ailuropoda–Stegodon* fauna from the Diaozhongyan Cave, Guangxi, South China. Quat Geochronol. 60:1–7. doi:10.1016/j.quageo.2020.101111.
Li DW, Hu CY, Wang W, Chen J, Tian F, Huang SM, Bae CJ. 2017. The stable isotope record in cervid tooth enamel from Tantang Cave, Guangxi: implications for the Quaternary East Asian monsoon. Quat Int. 434:156–162. doi:10.1016/j.quaint.2015.11.049.
Li YY, Pei SW, Tong HW, Yang CYJ XX, Liu W, Wu XJ. 2013. A preliminary report on the 2011 excavation at Houbeishan Fuyan Cave, Daoxian, Hunan Province. Acta Anthropol Sinica. 32(2):133–143. [in Chinese with English summary].
Liu W, Jin CZ, Zhang YQ, Cai YJ, Xing S, Wu XJ, Cheng H, Edwards RL, Pan WS, Qin DG, et al. 2010. Human remains from Zhirendong, South China, and modern human emergence in East Asia. Proc Natl Acad Sci. 107(45):19201–19206. doi:10.1073/pnas.1014386107
Liu X, Shen G, Tu H, Lu C, Granger DE. 2015. Initial $^{26}Al/^{10}Be$ burial dating of the hominin site Bailong Cave in Hubei Province, central China. Quat Int. 389:235–240. doi:10.1016/j.quaint.2014.10.028.
MacKinnon J. 1974. The behaviour and ecology of wild orang-utans (*Pongo pygmaeus*). Anim Behav. 22(1):3–74. doi:10.1016/S0003-3472(74)80054-0.
Maglio VJ. 1973. Origin and evolution of the elephantidae. Trans Am Phil Soc. 63(3):1–149. doi:10.2307/1006229.
Matthew W, Granger W. 1923. New fossil Mammals from the Pliocene of Szechuan. Bull Am Mus Nat Hist. 48:563–598.
Ma J, Wang Y, Jin C, Hu Y, Bocherens H. 2019. Ecological flexibility and differential survival of Pleistocene *Stegodon orientalis* and *Elephas maximus* in mainland Southeast Asia revealed by stable isotope (C, O) analysis. Quat Sci Rev. 212:33–44. doi:10.1016/j.quascirev.2019.03.021.
Ma J, Wang Y, Jin C, Yan Y, Qu Y, Hu Y. 2017. Isotopic evidence of foraging ecology of asian elephant (*Elephas maximus*) in south China during the late Pleistocene. Quat Int. 443:160–167. doi:10.1016/j.quaint.2016.09.043.
Nater A, Mattle-Greminger MP, Nurcahyo A, Nowak MG, de Manuel M, Desai T, Groves C, Pybus M, Sonay TB, Roos C, et al. 2017. Morphometric,

behavioral, and genomic evidence for a new orangutan species. Curr Biol. 27 (22):3487–3498. doi:10.1016/j.cub.2017.09.047
Nelson SV. 2014. The paleoecology of early Pleistocene *Gigantopithecus blacki* inferred from isotopic analyses. Am J Phys Anthropol. 155(4):571–578. doi:10.1002/ajpa.22609.
Nowak RM. 1999. Walker's Mammals of the World. London: The John Hopkins University Press.
Patte E. 1928. Comparaison des faunes de mammifères de Langson (Tonkin) et du SE Tchouen. Bulletin de la Société Géologique Française. 28:55–63.
Payne J, Prudente C. 2008. Orang-utans: behaviour, Ecology and Conservation. Wahroonga: New Holland Publishers.
Pei WC. 1935. Fossil mammals from the Kwangsi caves. Bull Geol Surv Can. 14:413–425.
Pei W. 1980. *Ailuropoda-Stegodon* Fauna. Journal of Guizhou Normal University (Social Science). 1:3–9.
Pope GG, Frayer DW, Liangchareon M, Kulasing P, Nakabanlang S. 1981. Palaeoanthropological investigations of the Thai-American expedition in northern Thailand (1978-1980): an interim report. Asian Perspect. 21 (2):147–163.
Pushkina D, Bocherens H, Chaimanee Y, Jaeger -J-J. 2010. Stable carbon isotope reconstructions of diet and paleoenvironment from the late Middle Pleistocene Snake Cave in Northeastern Thailand. Naturwissenschaften. 97 (3):299–309. doi:10.1007/s00114-009-0642-6.
Qiu Z. 2006. Quaternary environmental changes and evolution of large mammals in North China. Vertebr Palasiat. 44(2):109–132. [in Chinese with English summary].
Qu Y, Jin C, Zhang Y, Hu Y, Shang X, Wang C. 2014. Preservation assessments and carbon and oxygen isotopes analysis of tooth enamel of *Gigantopithecus blacki* and contemporary animals from Sanhe Cave, Chongzuo, South China during the Early Pleistocene. Quat Int. 354:52–58. doi:10.1016/j.quaint.2013.10.053.
Rink W, Wei W, Bekken D, Jones H. 2008. Geochronology of *Ailuropoda–Stegodon* fauna and *Gigantopithecus* in Guangxi Province, southern China. Quat Res. 69(3):377–387. doi:10.1016/j.yqres.2008.02.008.
Roth VL, Shoshani J. 1988. Dental identification and age determination in *Elephas maximus*. J Zool Lond. 214(4):567–588. doi:10.1111/j.1469-7998.1988.tb03760.x.
Schaller GB. 1967. The Deer and the Tiger: a Study of Wildlife in India. Chicago: The University of Chicago Press.
Schwartz JH, Long VT, Cuong NL, Kha LT, Tattersall I. 1994. A diverse hominoid fauna from the late Middle Pleistocene breccia cave of Tham Khuyen, Socialist Republic of Vietnam. Anthropol Pap Am Mus Nat Hist. 73:1–11.
Shao Q, Wang W, Deng C, Voinchet P, Lin M, Zazzo A, Douville E, Dolo JM, Falgueres C, Bahain JJ. 2014. ESR, U-series and paleomagnetic dating of *Gigantopithecus* fauna from Chuifeng Cave, Guangxi, southern China. Quat Res. 82(1):270–280. doi:10.1016/j.yqres.2014.04.009.
Shao Q, Wang Y, Voinchet P, Zhu M, Lin M, Rink WJ, Jin C, Bahain -J-J. 2017. U-series and ESR/U-series dating of the *Stegodon-Ailuropoda* fauna at Black Cave, Guangxi, southern China with implications for the timing of the extinction of *Gigantopithecus blacki*. Quat Int. 434:65–74. doi:10.1016/j.quaint.2015.12.016.
Si X, Liu J, Zhang H, Yuan C. 1993. Preliminary report on the excavation of Panxian, Dadong, a Paleolithic cave-site in Guizhou Province. Acta Anthropol Sinica. 12(2):113–119. [in Chinese with English summary].
Stacklyn S, Wang Y, Jin CZ, Wang Y, Sun F, Zhang C, Jiang S, Deng T. 2017. Carbon and oxygen isotopic evidence for diets, environments and niche differentiation of early Pleistocene pandas and associated mammals in South China. Palaeogeogr Palaeoclimatol Palaeoecol. 468:351–361. doi:10.1016/j.palaeo.2016.12.015.
Storm P, Aziz F, de Vos J, Kosasih D, Baskoro S, van den Hoek Ostende LW, van den Hoek Ostende LW. 2005. Late Pleistocene *Homo sapiens* in a tropical rainforest fauna in east java. J Hum Evol. 49(4):536–545. doi:10.1016/j.jhevol.2005.06.003.
Sun L, Deng CL, Wang W, Liu CC, Kong YF, Wu BL, Liu SZ, Ge JY, Qin HF, Zhu RX. 2017. Magnetostratigraphy of Plio-Pleistocene fossiliferous cave sediments in the Bubing Basin, southern China. Quat Geochronol. 37:68–81. doi:10.1016/j.quageo.2016.09.007.
Sun L, Wang Y, Liu C, Zuo T, Ge J, Zhu M, Jin C, Deng C, Zhu R. 2014. Magnetochronological sequence of the Early Pleistocene *Gigantopithecus* faunas in Chongzuo, Guangxi, southern China. Quat Int. 354:15–23. doi:10.1016/j.quaint.2013.08.049.
Suraprasit K, Jaeger JJ, Chaimanee Y, Chavasseau O, Yamee C, Tian P, Panha S. 2016. The Middle Pleistocene vertebrate fauna from Khok Sung (Nakhon Ratchasima, Thailand): biochronological and paleobiogeographical implications. Zookeys. 613:1–157. doi:10.3897/zookeys.613.8309.
Suraprasit K, Jaeger JJ, Chaimanee Y, Sutcharit C. 2021. Taxonomic reassessment of large mammals from the Pleistocene *Homo*-bearing site of Tham Wiman Nakin (Northeast Thailand): relevance for faunal patterns in mainland Southeast Asia. Quat Int. 603:90–112. doi:10.1016/j.quaint.2020.06.050.
Suraprasit K, Jongautchariyakul S, Yamee C, Pothichaiya C, Bocherens H. 2019. New fossil and isotope evidence for the Pleistocene zoogeographic transition and hypothesized savanna corridor in peninsular Thailand. Quat Sci Rev. 221:1–23. doi:10.1016/j.quascirev.2019.105861.
Swindler DR. 2002. Primate Dentition: an Introduction to the Teeth of Non-human Primates. Cambridge: Cambridge University Press.
Takai M, Zhang Y, Kono RT, Jin C. 2014. Changes in the composition of the Pleistocene primate fauna in southern China. Quat Int. 354:75–85. doi:10.1016/j.quaint.2014.02.021.
Tong H. 2004. Tapiridae. In: Zheng S, editor. Jianhsi hominid Site. Beijing: Science Press; p. 233–250.
Tong H. 2005. Dental characters of the Quaternary tapirs in China, their significance in classification and phylogenetic assessment. Geobios. 38 (1):139–150. doi:10.1016/j.geobios.2003.07.006.
Tong H, Deng L, Chen X, Zhang B, Wen J. 2018a. Late Pleistocene proboscideans from Yangjiawan caves in Pingxiang of Jiangxi, with discussions on the *Stegodon orientalis-Elephas maximus* assemblage. Vertebr Palasiat. 56 (4):306–326. [in Chinese with English summary].
Tong H, Guérin C. 2009. Early Pleistocene *Dicerorhinus sumatrensis* remains from the Liucheng *Gigantopithecus* Cave, Guangxi, China. Chin Sci Bull. 42 (4):525–539.
Tong H, Wu X, Dong Z, Sheng J, Jin Z, Pei S, Liu W. 2018b. Preliminary report on the mammalian fossils unearthed from the ancient human site of Hualong Cave in DongZhi, Anhui. Acta Anthropol Sin. 37: 284–305. in Chinese with English summary.
Tong H, Zhang B, Wu X, Qu S. 2019. Mammalian fossils from the Middle Pleistocene human site of Bailongdong in Yunxi, Hubei. Acta Anthropol Sinica. 38(4):613–640.
Tougard C 1998. Les faunes de grands mammifères du Pléistocène moyen terminal de Thaïlande dans leur cadre phylogénétique, paléoécologique et biochronologique. PhD. Thesis. University Montpellier II, Montpellier.
Tougard C, Montuire S. 2006. Pleistocene paleoenvironmental reconstructions and mammalian evolution in South-East Asia: focus on fossil faunas from Thailand. Quat Sci Rev. 25(1–2):126–141. doi:10.1016/j.quascirev.2005.04.010.
Van den Bergh GD. 1999. The late Neogene elephantoid-bearing faunas of Indonesia and their palaeozoogeographic implications: a study of the terrestrial faunal succession of Sulawesi, Flores and Java, including evidence for early hominid dispersal east of Wallace's Line. Scripta Geologica. 117:1–419.
Van den Bergh GD, de Vos J, Sondaar PY. 2001. The Late Quaternary palaeogeography of mammal evolution in the Indonesian Archipelago. Palaeogeogr Palaeoclimatol Palaeoecol. 171(3–4):385–408. doi:10.1016/S0031-0182(01)00255-3.
van der Made J. 1996. Listriodontinae (Suidae, Mammalia), their evolution, systematic, and distribution in time and space. Contrib to Tertiary and Quat Geol. 33:3–254.
Wang W. 2005. Early Pleistocene Hominoid fossil assemblage from Mohui Cave,Tiandong county, Guangxi, South China and its significance of early human evolution. Thesis of China University of Geoscience.
Wang Y, Jin C, Pan W, Qin D, Yan Y, Zhang Y, Liu J, Dong W, Deng C. 2017a. The Early Pleistocene *Gigantopithecus-Sinomastodon* fauna from Juyuan karst cave in Boyue Mountain, Guangxi, South China. Quat Int. 434:4–16. doi:10.1016/j.quaint.2015.11.071.
Wang W, Liao W, Li D, Tian F. 2014. Early Pleistocene large-mammal fauna associated with *Gigantopithecus* at Mohui Cave, Bubing Basin, South China. Quat Int. 354(354):122–130. doi:10.1016/j.quaint.2014.06.036.
Wang L, Lin Y, Chang S, Yuan J. 1982. Mammalian fossils found in northwest part of Hunan Province and their significance. Vertebr Palasiat. 20 (4):350–358. [in Chinese with English summary].
Wang W, Potts R, Baoyin Y, Huang WW, Cheng H, Edwards RL, Ditchfield P. 2007. Sequence of mammalian fossils, including hominoid teeth, from the Bubing Basin caves, South China. J Hum Evol. 52(4):370–379. doi:10.1016/j.jhevol.2006.10.003.
Wang W, Potts R, Hou YM, Chen YF, Wu HY, Yuan BY, Huang WW. 2005. Early Pleistocene hominid teeth recovered in Mohui cave in Bubing Basin, Guangxi, South China. Chin Sci Bull. 50(23):2777–2782. doi:10.1360/982004-614.
Wang Y, Zhao L, Du B, Zhang L, Wang X, Cai H. 2017b. New proboscidean remains associated with *Homo sapiens* from the Mawokou Cave in Bijie, Guizhou Province of south-western China. Acta Anthropol Sinica. 36 (3):414–425. in Chinese with English summary.
Wattanapituksakul A 2016. Diversity and Diet of Middle to Late Pleistocene Bovid Assemblages in Thailand. Ph. D. Thesis. Mahasarakarm University, MahaSarakarm.
Wattanapituksakul A, Filoux A, Amphansri A, Tumpeesuwan S. 2018. Late Pleistocene Caprinae assemblages of Tham Lod Rockshelter (Mae Hong

Son Province, Northwest Thailand). Quat Int. 493:212–226. doi:10.1016/j.quaint.2018.06.003.
Wu XJ, Pei SW, Cai YJ, Tong HW, Li Q, Dong Z, Sheng JC, Jin ZT, Ma DD, Xing S, et al. 2019. Archaic human remains from Hualongdong, China, and Middle Pleistocene human continuity and variation. Proc Natl Acad Sci. 116 (20):9820–9824. doi:10.1073/pnas.1902396116
Yan Y 2016. Systematic research on *Rhinoceros* from the Quaternary of Southern China. Ph. D. Thesis. The Univerity of Chinese Academy of Sciences, Beijing.
Yan Y, Wang Y, Jin C, Mead JI. 2014. New remains of *Rhinoceros* (Rhinocerotidae, Perissodactyla, Mammalia) associated with *Gigantopithecus blacki* from the Early Pleistocene Yanliang Cave, Fusui, South China. Quat Int. 354:110–121. doi:10.1016/j.quaint.2014.01.004.
Zeitoun V, Chinnawut W, Debruyne R, Auetrakulvit P. 2015. Assessing the occurrence of the *Stegodon* and *Elephas* in China and Southeast Asia during the Early Pleistocene. Bull Soc Géol France. 6:85–101.
Zeitoun V, Chinnawut W, Debruyne R, Frère S, Auetrakulvit P. 2016. A sustainable review of the Middle Pleistocene benchmark sites including the *Ailuropoda–Stegodon* faunal complex: the Proboscidean point of view. Quat Int. 416:12–26. doi:10.1016/j.quaint.2015.09.045.
Zeitoun V, Chinnawut W, Lenoble A, Bochaton C, Burdette K, Thompson J, Mallye JB, Frère S, Debruyne R, Antoine PO, et al. 2019. Dating, stratigraphy and taphonomy of the Pleistocene site of ban Fa Suai II (northern Thailand): contributions to the study of paleobiodiversity in Southeast Asia. Ann Paleontol. 2(105):275–285. doi:10.1016/j.annpal.2019.03.005.
Zeitoun V, Seveau A, Forestier H, Thomas H, Lenoble A, Laudet F, Antoine PO, Debruyne R, Ginsburg L, Mein P. 2005. Découverte d'un assemblage faunique à *Stegodon–Ailuropoda* dans une grotte du Nord de la Thaïlande (Ban Fa Suai, Chiang Dao). Comptes Rendus Palevol. 4(3):255–264. doi:10.1016/j.crpv.2004.11.013.
Zhang B, Chen X, Tong HW. 2018. Tooth remains of Late Pleistocene moschid and cervid (Artiodactyla, Mammalia) from Yangjiawan and Fuyan Caves of southern China. Quat Int. 490:21–32. doi:10.1016/j.quaint.2018.05.036.
Zhang J, Huang W, Hu Y, Yang S, Zhou L. 2015. Optical dating of flowstone and silty carbonate-rich sediments from Panxian Dadong Cave, Guizhou, southwestern China. Quat Geochronol. 30:479–486. doi:10.1016/j.quageo.2015.01.011.
Zhang Y, Jin C, Cai Y, Kono R, Wang W, Wang Y, Zhu M, Yan Y. 2014. New 400-320 ka *Gigantopithecus blacki* remains from Hejiang Cave, Chongzuo City, Guangxi, South China. Quat Int. 354:35–45.Zhang. doi:10.1016/j.quaint.2013.12.008.
Zhang Z, Liu J, Zhang H, Yuan C. 1997. A Pleistocene mammalian fauna from Panxiandadong, Guizhou Province. Acta Anthropol Sinica. 16(3):209–220.
Zhang YY, Wu ML, Liu JR. 1973. *Gigantopithecus* teeth discovered in Wuming, Kwangsi. Chin Sci Bull. 18(3):130–133.
Zheng S. 2004. Jianshi Hominid Site. Beijing: Science Press. [in Chinese with English summary].
Zheng Z, Lei Z. 1999. A 400,000 year record of vegetational and climatic changes from a volcanic basin, Leizhou Peninsula, southern China. Palaeogeogr Palaeoclimatol Palaeoecol. 145(4):339–362. doi:10.1016/S0031-0182(98)00107-2.
Zhou M. 1957. The nature and contrast of Tertiary and Early Quaternary mammalian fauna in South China. Chin Sci Bull. 13:394–400.